Optimization of the Active Magnetic Regenerator Refrigeration System

January 2014

Li Jing

Graduate School of Engineering

CHIBA UNIVERSITY

（千葉大学審査学位論文）

Optimization of the Active Magnetic Regenerator Refrigeration System

January 2014

Li Jing

Graduate School of Engineering

CHIBA UNIVERSITY

Optimization of the Active Magnetic Regenerator Refrigeration System

by

Li Jing

Submitted to the Department of Mechanical Engineering
on Jan 28, 2014, in partial fulfillment of the
requirements for the degree of
DOCTOR OF PHILOSOPHY in the Department of Mechanical Engineering

Abstract

Magnetic refrigeration is considered to be a future technology which does not use a fluorocarbon working fluid and has an energy saving potential. Although the improvement of magnetic refrigeration has been realized, there are no commercial devices available. The discovery of big MCE material is required. Meanwhile, the cooling system design, especially the important part regenerator, should be optimized. This thesis is focusing on the optimization of regenerator from geometry design and multi-layered regenerator ways. One and two dimensional models have been developed. The created models have been used to analysis the regenerator. Three most popular regenerators have been compared with Entropy generation minimization (EGM) method which is used to optimize the real devices and processes. The results present that flat plate regenerator has the best performance in the three regenerators. However, it is still required to be improved in the future for the limited heat transfer surface. The analysis of multi-layered regenerator presents a problem that even same total MCE generated by magnetic material will lead to a different performance for the different selection and arrangement of magnetic material. The most popular multi-layered regenerator is Iso-entropy change regenerator. However, according to the theoretical speculation, an idea entropy curve regenerator exists. A single material regenerator, Iso-entropy change regenerator and idea entropy curve regenerator have been compared. The results show that the idea entropy curve regenerator has a potential to be the most efficient one. The concept of idea entropy curve regenerator will be analyzed experimentally.

Thesis Supervisor: Nakagome Hideki
Title: Professor

Contents

List of Figures

List of Tables

Chapter 1

Introduction

Refrigeration is very important for our life and health. Applications including refrigerator, air conditioning, cooling system for vehicle, and plant fridges etc. Based on the conventional refrigeration technology, 30 % electricity has been consumed. While, magnetic refrigeration (MR) is considered to be a future technology for its energy saving potential. The efficiency of magnetic refrigeration can theoretically reach 30%-60% of Carnot cycle, whereas the efficiency of vapor compression refrigeration is only 5%-10% of Carnot cycle [24]. MR makes use of the magnetocaloric effect (MCE). It is an environmentally attractive alternative to vapor compression refrigeration as it does not use a fluorocarbon working fluid. Therefore, it exhibits no Ozone Depletion Potential (ODP). Also Global Warming Potential (GWP) is usually very small for a definition of these broadly accepted measures [16]. Moreover, the magnetic refrigeration system can be design to be more compact, because of the higher entropy density of magnetic material compared with that of refrigerant gas.

1.1 Background

In 1881, Magnetocaloric effect (MCE) discovered by Warburg in iron. Debye (1926) [6] and Giauque (1927) [9] proposed to use reversible temperature change in paramagnetic salts to obtain low temperatures by adiabatic demagnetization) [10]. The first experiments to realize this idea were in 1930s. This cooling technology was first

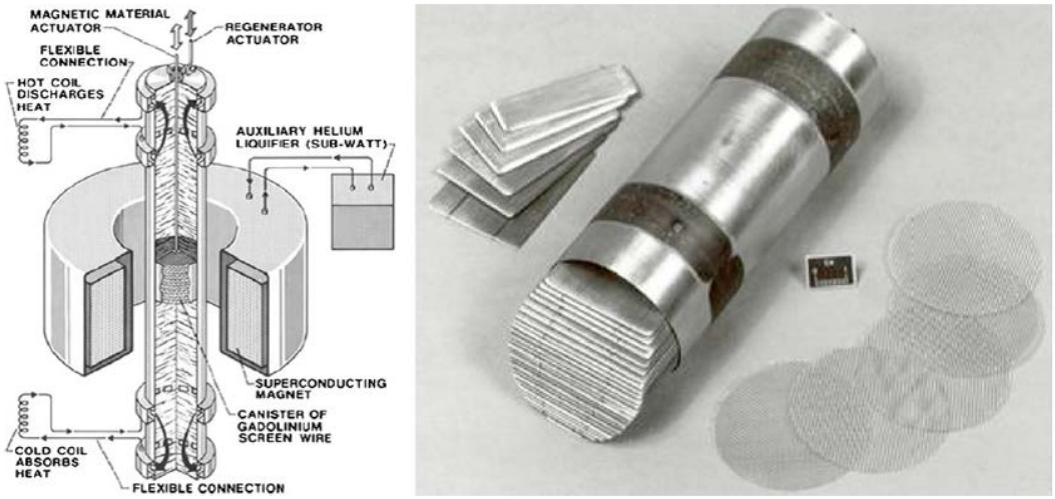

Figure 1-1: First room-temperature magnetic heat pump designed by G. V. Brown [3]

demonstrated experimentally by chemist Nobel Laureate William F. Giauque and his colleague D. P. MacDougall in 1933 for cryogenic purposes when they reached 0.25 K[] . This technology was used in low temperature. Applications include Adiabatic Demagnetization Refrigerator (ADR) and nuclear demagnetization refrigeration (NDR) etc. In 1975, a breakthrough with Brown‘s work. He built the first near room temperature magnetic heat pump which is showed in Figure 1-1. It used Gd plates as the magnetic material and 7 tesla magnetic field getting 14 K temperature rise under adiabatic condition [3].

In 1983, Barclay suggested the active magnetic regenerator (AMR) refrigeration cycle, which is based on the Brayton cycle [2]. In this cycle the magnetic material serves not only as a refrigerant but also as a regenerator. It makes the larger temperature span can be realized. In 1992, Chen et al. concluded that a regenerative cycle is more efficient than the Carnot, Ericsson or Stirling cycles.

In 1997, two key developments enhanced the feasibility for producing a magnetic refrigerator for near room temperature commercial use. First, Prof.Pecharsky and Gschneidner have reported the discovery of the so-called ”giant” Magnet caloric effect (MCE) [14]. It was observed in Gd alloys, most notably Gd5Si2Ge2 which has 50% higher entropy change than just Gd. Secondly, Prof. Karl A. Gschneidner, Jr. built the Ames Laboratory /Astronautics proof-of-principle refrigerator system

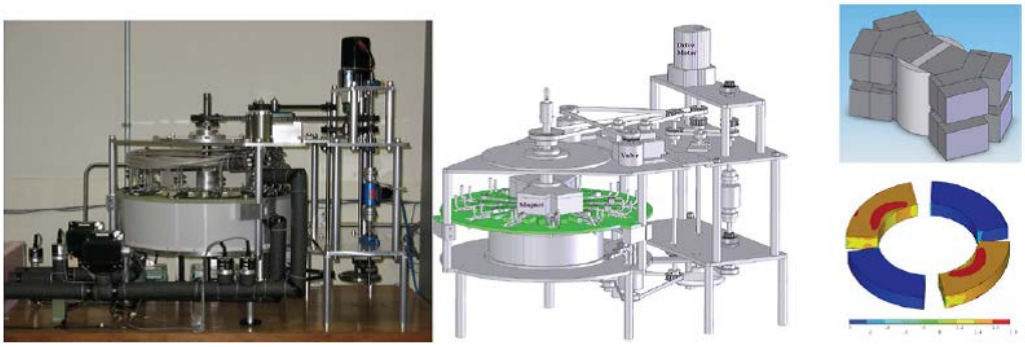

Figure 1-2: Rotary magnetic refrigerator built by Astronautics Corporation of America [25]

showed that magnetic refrigeration was competitive with conventional gas compression cooling. The system used the Gd spheres and Ericcson cycle systems that had lasted 1500 hours as of mid-1998, and had run maintenance free [4]. These developments attracted interest from scientists and companies worldwide who started developing new kinds of room temperature materials and magnetic refrigerator designs. Lots of refrigeration systems had been built which used superconducting magnet and operate in low frequency. Until 2001, the worlds first rotary magnetic refrigerator with permanent magnets built by Zimm and his collaborators at the Astronautics Corporation of America [25]. Figure 1-2 showed this system. A higher frequency of operation 4Hz, 1.5T permanent magnets and the rotary magnetic refrigerator principle had been used. It marked the transition between the first and the second generation of room temperature magnetic refrigeration and heat pump technologies. After that, the numbers of patents per year for room temperature magnetic refrigeration grow up dramatically.

1.2 Problem description

Comparing to conventional refrigeration technology, magnetic refrigeration is a more complex technology. It relies on the MCE and uses solid material as a refrigerant .Water or other water based on liquids are the heat transfer fluid which will change heat between inside system and outside environment. Although the improvement of

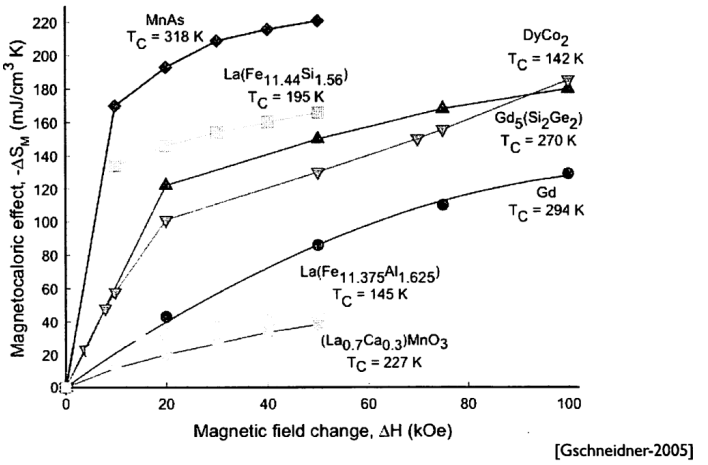

Figure 1-3: Magnetic materials used near room temperature

magnetic refrigeration has been realized, there are no commercial devices available. Main problems lie in:

1.2.1 Large MCE and cheap material in a wild operation temperature

The magnetic materials are mainly Gd, GdSiGe alloys, MnAs-like materials, perovskite-like materials which can be seen in Figure 1-3. The MCE of these materials is no more a few degrees in a magnetic field of one tesla [24]. In a wild operation temperature span like 40 kelvin for room temperature, MCE decrease very quickly when the temperature deviates curie temperature which can be seen in Figure1-41-5. The large MCE material in a wild operation temperature is required. What more is, these rare earth materials are very expensive which do not meet the requirement of commercialization. Once cheap and high performance magnetic materials are found, the breakthrough of magnetic refrigeration will be achieved.

1.2.2 Excellent heat transfer of regenerator and heat exchanger

Currently the lab devices have shown poor efficiency, largely due to viscous losses, thermal conductivity losses, heat exchanger losses and ineffective hydraulic design

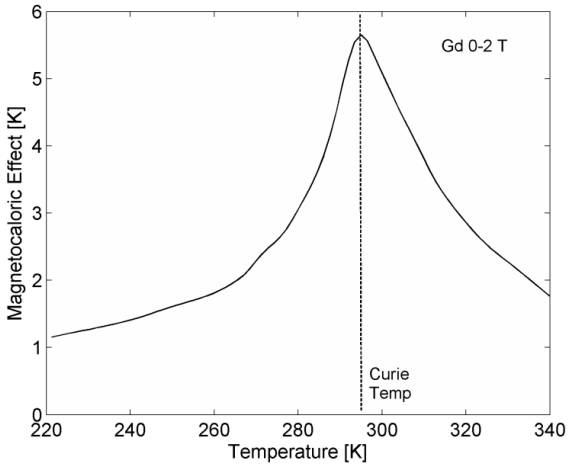

Figure 1-4: Magnetocaloric effect of Gd for a 0-2 T applied field change [21]

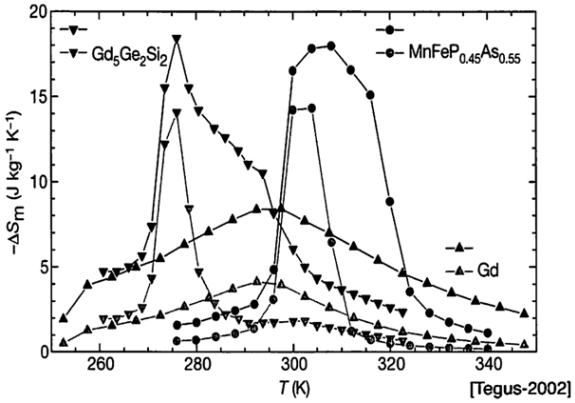

Figure 1-5: Giant magnetic material $Gd_5Ge_2Si_2$ with a narrow operational temperature span

etc. Theoretically, there is still space for the improvement of MR device design. One of the key points is the optimization of regenerator which includes the mechanical design, structural design (porous media, flat plates, wire-screens, and so on), multilayer regenerator design etc. Moreover, the selection of heat transfer fluid also should be considered. Water or water based on fluid is wildly used. However water has a huge heat capacity which is a negative effect for the performance. In conclusion, the work done by the magnetic material should be used as efficient as it can be.

1.2.3 Low cost, compact and strong permanent magnet

For low temperature applications, 5 to 7 Tesla superconductor magnets have been used which are expensive and structure-complicate. It is not impractical to use it in a commercial room temperature MR system. Neodymium magnets (NdFeB) which are the strongest type of permanent magnet made have been used wildly in recently years in MR lab devices. However, it is too expensive and only produces no more than 1.5 Tesla. The supply of magnetic field is also a problem need to be solved.

1.2.4 Multidisciplinary nature of MR research

It is crucial to underline the multidisciplinary nature of MR research. MR research needs the cooperation in the fields of fundamental physics, mechanical and material engineering, even computer science. Mechanical scientists have to understand the phenomenal of heat transfer, fluid dynamics, and how does the entropy change of magnetic material will influence the cooling efficiency. Then, they can optimize the heat transfer and discuss with the material experts what the idea magnetic material is. Solid physicist or material experts will focus on the discovery of large MCE material and also they want to know the feedback of magnet-caloric material performance in cooling device. Moreover computer experts can help build a more complex model which can be accurately and quickly simulate the materials as well as the operation of the cooling system. Although there are some difficulties in interdisciplinary cooperation, good cooperation may lead to great breakthroughs.

1.3 Motivation and Objective

As we mentioned in chapter 1-2-2, theoretically, there is still requirement for the improvement of MR device design. In order to improve the MR device, it is crucial to deeply understand the physical phenomenon of heat transfer, fluid dynamics and minimize the mechanical losses.Thus, a reliable numerical model is required. It can analyze the complicated parameters (frequency, mass flow rate et.) and also help to predict the performance of MR system. Until now, the 1-dimensional numerical model is used in many investigators such as Engelbrecht et al. [5] and Viallet, D [13].It based on the determination of the convective heat transfer coefficient between magnetic material and heat transfer fluid and the friction factor to specify the pressure drop in the fluid due to viscosity. However, considering the unignorable factors in previous studies, heat transfer between the regenerator and outside air in room MR system must be taken account into the practical model. And to eliminate the use of heat transfer and pressure drop correlations, the velocity, pressure and temperature field must to be solved simultaneously. In doing so, a 2-dimentional model close to reality is needed to be modeled.

To minimize the mechanical losses and efficiently make use of MCE, it is crucial to optimize the most important part regenerator of for room temperature MR system. We consider using two main optimization ways for the regenerator. One is the multi-layered regenerator which can realize a big MCE in a wild temperature span with several magnetic materials carefully layer on the regenerator. Another is the geometry design of regenerator. A good geometry design will reduce the heat losses and improve the efficiency.

Until now, the geometry have been limited to flat plate and packed sphere design. In recent years, the micro-channel regenerator is also considered to be a potential candidate regenerator design for the high rate of heat and mass transfer. However, it is not clear that which can be the most efficient in three kinds of regenerators. Few papers actually focus on it, both from theoretical and experimental point of review. The comparing and numerically analyze of the three regenerators, parallel-plate, packed-

bed and Micro-channel regenerator, haven't been discussed. This thesis will compare and discuss the detail of heat process in three regenerators numerically. Based on the discussion of comparison, the suggestions of optimized regenerator geometries design for magnetic refrigeration systems will be given.

Another problem we mentioned in chapter 1-2-1 is that we have not found a idea material which has a big MCE in a wild operation temperature span. The MCE material we used even has a big MCE at curie temperature. However, the MCE decrease very quickly when the temperature deviates curie temperature. Thus, Recently years, multi-layered regenerator is becoming a hot topic and showed a potential to improve the performance [8] [9] [12]. It is considered that several materials will be carefully layered on the regenerator which can realize a big MCE in a wild temperature span. However, very few papers [16] actually discussed the thermodynamic requirement of multi-layer regenerator. which is crucial for the correct selection and arrangement of the materials used. The investigation of multi-layered regenerator is required from both experimental and simulation point of view. This thesis will perform an analyze of thermodynamic requirement and optimize the multi-layered way. Once the optimization way is found, real materials can be selected and arranged in the regenerator to best fit it.

1.4 Dissertation Organization

The rest of this dissertation is organized as follows. In the next chapter the principles of MCE, and thermal cycle are introduced. Thermal cycle includes Ericson, Bryton and AMR cycle. Chapter 3 constructs models of the AMR system and shows the parameter simulation results in room temperature. Chapter 4 and 5 contains the two main optimization ways of regenerator, geometry and multi-layer design. Its main purpose is to enhance the heat transfer insider regenerator and maximize the work from MCE material. Chapter 6 is a outlines conclusions and future work.

Chapter 2

Fundamental of Magnetic Refrigeration system

In this chapter the main terms and conceptions about Magnetic refrigeration system are introduced. The thermodynamic approaches and the main cycles are considered.

2.1 Magnetocaloric effect (MCE)

The magnetocaloric effect (MCE) is a magneto thermodynamic phenomenon in which a reversible change in temperature of a suitable material is caused by exposing the material to a changing magnetic field . This is also known by low temperature physi-

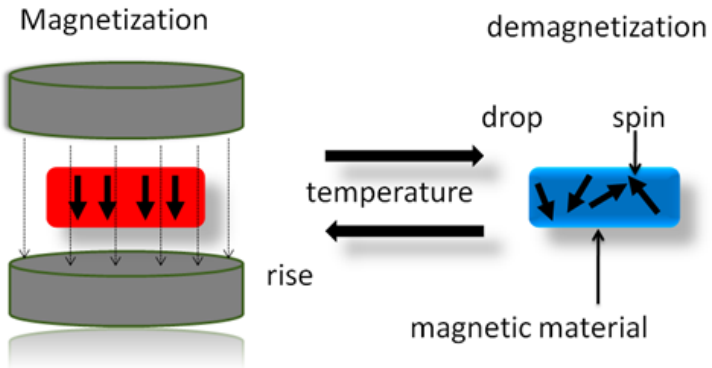

Figure 2-1: Magnetocaloric effect

cists as adiabaticdemagnetization, due to the application of the process specifically to create a temperature drop. In that part of the overall refrigeration process, a decrease in the strength of an externally applied magnetic field allows the magnetic domains of a chosen (magnetocaloric) material to become disoriented from the magnetic field which is also showed in Figure 2-1. by the agitating action of the thermal energy (phonons) present in the material. If the material is isolated so that no energy is allowed to (re)migrate into the material during this time, i.e., an adiabatic process, the temperature drops as the domains absorb the thermal energy to perform their reorientation. The randomization of the domains occurs in a similar fashion to the randomization at the curie temperature, except that magnetic dipoles overcome a decreasing external magnetic field while energy remains constant, instead of magnetic domains being disrupted from internalferromagnetism as energy is added.

2.2 General thermodynamic approach of magnetic refrigeration

The main terms and conceptions about the thermodynamic approach of cyclic magnetic refrigeration processes are presented. The main objective of this part is to yield a theoretical basis for an optimal design of new magnetic refrigeration and heat pump devices. The thermodynamics of magnetic refrigeration is introduced by the first law of thermodynamics1:

$$dQ = dU + dW \tag{2.1}$$

where dU is the infinitesimal change of the internal energy. dQ is a small amount of heat added to or removed from the considered system, or created by a magnetic internal source (magnetocaloric effect). dW denotes the differential of the work performed on the system, or extracted from it. To obtain the specific (volumetric) energy equation , the work in the magnetic material, a equation is considered as follow (a

more detailed derivation is found in Landau and Lifshitz):

$$dw = -\overrightarrow{H}d\overrightarrow{B} \tag{2.2}$$

Reversibly performed or extracted work leads to this alteration of the specific energy of the magnetic system (specimen and surrounding magnetic field to infinity). The induction dB is a combination of stress dH and order parameter dM and defined by:

$$B = \mu_0(\overrightarrow{H} + \overrightarrow{M}) \tag{2.3}$$

with the magnetic permeability 0 of the vacuum. This equation is inserted into Equation 2.2 to become:

$$dw = -\mu_0\overrightarrow{H}d\overrightarrow{M} - \frac{\mu_0}{2}d(\overrightarrow{H^2}) \tag{2.4}$$

In Equation 2.4 the first term describes the specific energy in the specimen and the second, which can be written by introducing a potential:

$$\phi = \frac{1}{2}\overrightarrow{H^2} \tag{2.5}$$

denotes the specific energy in the magnetic field. dH defines a conservative field with the potential f. It then follows that:]

$$dw = -\mu_0\overrightarrow{H}d\overrightarrow{M} - \mu_0 d\phi \tag{2.6}$$

At this stage the last term is often neglected with the argument that it does not apply in cyclic processes.

We now consider the differential of the redefined internal energy $\mu_1(s, m)$:

$$d\mu_1 = dq + dw_1 = (\frac{\partial\mu_1}{\partial s})_m ds + (\frac{\partial\mu_1}{\partial m})_s dm \tag{2.7}$$

Because the volume is also constant, it is written:

$$(\frac{\partial \mu_1}{\partial s})_m = (\frac{\partial \mu_1}{\partial s})_(mv) = (\frac{\partial \mu_1}{\partial s})_v = T \tag{2.8}$$

It is known from the conventional thermodynamics of gas compression that the derivative of the internal energy in terms of the entropy is identical to the temperature, and this is therefore not proven here. Comparing Equation 2.7 and taking equation 2.8 into consideration, it follows that:

$$dq = Tds \tag{2.9}$$

a well-known relation for reversible processes. By inserting Equation 2.9 into Equation 2.7, it follows for the specific internal energy:

$$d\mu_1 = Tds - \mu_0 \overrightarrow{H} d\overrightarrow{M} \tag{2.10}$$

Using this relationship between entropy, internal energy, and magnetic work, it becomes possible to apply all of the typical thermodynamic results and identities that are ordinarily used in the context of a pure compressible substance to a magnetocaloric material.

Magnetic refrigerator completes cooling by magnetic material through magnetic refrigeration cycle. In general a magnetic refrigeration cycle consists of magnetization and demagnetization in which heat is expelled and absorbed respectively, and two other benign middle processes.

2.3 Thermal cycle

The basic cycles for magnetic refrigeration are magnetic Carnot cycle, magnetic Stirling cycle, magnetic Ericsson cycle and magnetic Brayton cycle, among which the magnetic Ericsson and Brayton cycles are applicable for room temperature magnetic refrigeration for the Ericsson and Brayton cycles employ a regenerator to achieve a

large temperature span and are easy to operate. In order to understand magnetic refrigeration deeper, some concepts necessary are introduced. According to the first law of thermodynamics, in a idea refrigeration cycle, the relationship between the heat Q_h rejected to hot exchanger (at temperature T_h), the heat absorbed from cold exchanger (at temperature T_c), the input work W_i as follows:

$$Q_c = Q_h - W_i \tag{2.11}$$

Q_h ,Q_c ,W_i are related to heat rejection $\dot{Q}_h$, cooling capacity $\dot{Q}_c$ and work rate $\dot{W}_i$in refrigerator as follows:

$$\dot{Q}_h = Q_h \nu \tag{2.12}$$

$$\dot{Q}_c = Q_c \nu \tag{2.13}$$

$$\dot{W}_i = W_i \nu \tag{2.14}$$

where ν is the operation frequency of the regenerator. For isothermal reversible heat transfer, the corresponding entropy change at hot (ΔS_h) and cold (ΔS_c) ends can be determined as follows:

$$\Delta S_h = \frac{Q_h}{T_h} \tag{2.15}$$

$$\Delta S_c = \frac{Q_c}{T_c} \tag{2.16}$$

The second law of thermodynamics requires that

$$\Delta S_h + \Delta S_c \geq 0 \tag{2.17}$$

The coefficient of performance (COP) is determined by the ratio between cooling capacity $\dot{Q}_c$ and power input $\dot{W}_i$. In an ideal cycle, the COP is the Carnot value:

$$COP_{carnol} = \frac{T_c}{T_h - T_c} \tag{2.18}$$

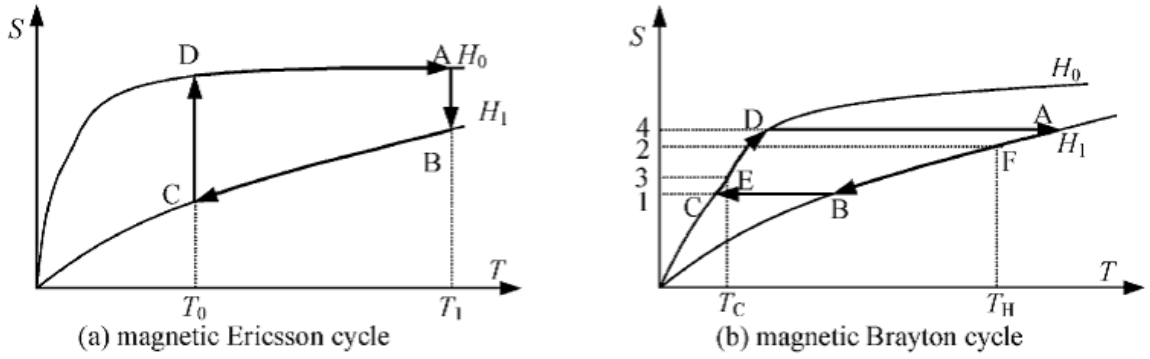

Figure 2-2: Magnetic refrigeration cycle

2.3.1 Ericsson and Brayton cycle

Figure 2-2 (a) illustrates magnetic Ericsson cycle which consists of two isothermal processes/ stages and two isofield processes. 1. Isothermal magnetization process I [(A-B in Figure 2-2(a)] When magnetic field increases from H_0 to H_1, the heat transferred from magnetic material to heat transfer fluid, makes the upper fluid increase in temperature. 2. Isofield cooling process II [B-C in Figure 2-2 (a)] In constant magnetic field of H1, heat transfer fluid moves downward to bottom and hence heat Q_{bc} which transferred from magnetic material to heat transfer fluid. Then a temperature gradient is set up in the regenerator. 3. Isothermal demagnetization process III [C-D in Figure 2-2(a)] When magnetic field decreases from H1 to H0, the magnetic material absorbs heat Q_{cd} from the lower heat transfer fluid. After that, the fluid decreases in temperature. 4. Isofield heating process IV [D-A in Figure 2-2(a)] In the field of H0, heat transfer fluid moves upward to the top and absorbs heat Q_{da}. According to the second law constraint, to make the Ericsson cycle possess the efficiency of magnetic Carnot cycle, it is required that the heat transferred in two isofield processes Q_{bc}, Q_{da} are equal each other. For an ideal Ericsson cycle, parallel TS curves are optimal, that keeps constant in the cooling temperature range. However, the current single magnetic materials cannot meet the requirement; so perfect regeneration of Ericsson cycle can only be realized by composite materials.

Magnetic Brayton cycle consists of two adiabatic processes and two isofield processes as shown in Figure 2-2 (b). In this cycle magnetization is accomplished adia-

batically, in contrast to the Ericsson cycle. The magnetic refrigerant cycles between the magnetic field of H0 and H1, and the temperature of high and low temperature heat source T_h and T_c, respectively. During the isofield cooling process F-A (constant magnetic field of H_1), magnetized material is set in thermal contact with the hot exchanger and is cooled back to the temperature Th (point F in Figure 2-2(b)). Further cooling from Th to Tc is accomplished with the help of a regenerator (form F to B in Figure 2-2 (b)). In total process A-B, it expels heat of the area of AB14 as Figure 2-2 (b) indicates. During the isofield heating process C-D (constant magnetic field H_0), magnetic refrigerant absorbs heat of the area of DC14. No heat flows from and out of the magnetic refrigerant in the adiabatic magnetization process D-A and the adiabatic demagnetization B-C process. Q_c, Q_h, W_i in Brayton cycle are reprensented by areas 1CE3, 2FA4,and ABCD, respectively. It should be noted that Brayton cycle is characterized by less refrigeration capacity and lager heat rejection in conparison with Ericcson cycle. But in real process, the differences between real Ericsson and Bryton cycles are small for deviation from true isothermal and adiabatic magnetization ([5]).

There is one more magnetic refrigeration cycle - active magnetic regenerator refrigeration (AMR) cycle, which is based on the Bryton cycle. In AMR cycle, magnetic material serves not only as a refrigerant but also as a regenerator. This cycle will be discussed more thoroughly below.

2.3.2 AMR cycle

In AMR magnetic material serves not only as a refrigerant providing temperature change as a result of adiabatic magnetization or demagenetization, but also as a regenerator for heat transfer fluid. One of the first constructions of magnetic refrigerator using AMR principle was suggested by van Geuns (1968). Figure 2-3 illustrates a schematic of an AMR. A typical AMR should include the following parts: a magnet, regenerator bed with magnetic material, hot and cold heat exchangers, and a displacer or other device providing heat transfer fluid flow back and forth through the regenerator bed.

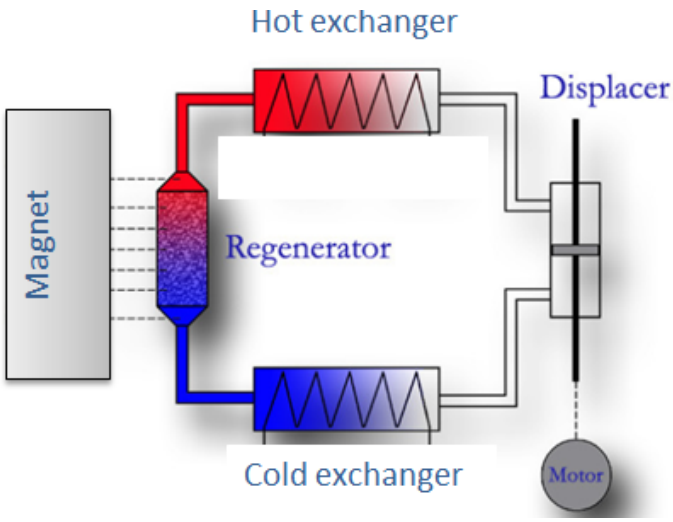

Figure 2-3: A schematic drawing of an AMR

Magntic brayton cycle (Figure 2-4) is the most basic one used in AMR cycle, which consists of two adiabatic processes and two constant magnetic field processes. The four steps in this cycle which are showed in Figure 2-5 are described as follows:

1) Process 1 to 2 is an adiabatic magnetization: The magnetic material is placed in adiabatic condition, and the heat transfer fluid doesnt flow. After magnetization, the temperature is up to $(T + \Delta T_{ad})$ due to the MCE.

2) Process 2 to 3 is fluid flowing from cold to hot at B=Bmax. The fluid rejects heat to hot exchanger. Then, the temperature of magnetic material is back to T.

3) Process 3 to 4 is an adiabatic demagnetization. The magnetic material is in another adiabatic condition where the magnet filed changes from Bmax ¿0 to Bmin=0, and the fluid doesnt flow. After demagnetization, the temperature is down to $(T - \Delta T_{ad})$.

4) Process 4 to 1 is fluid flowing from hot to cold at $B = B_{min}$. Pushing the fluid back from hot end to cold end, makes the temperature back to T, absorbing heat from cold exchanger.

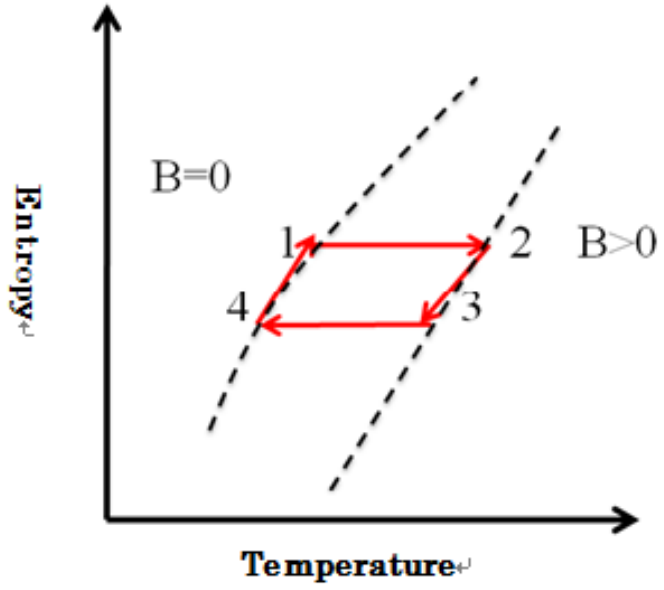

Figure 2-4: Entropy-temperature diagram for a one-short

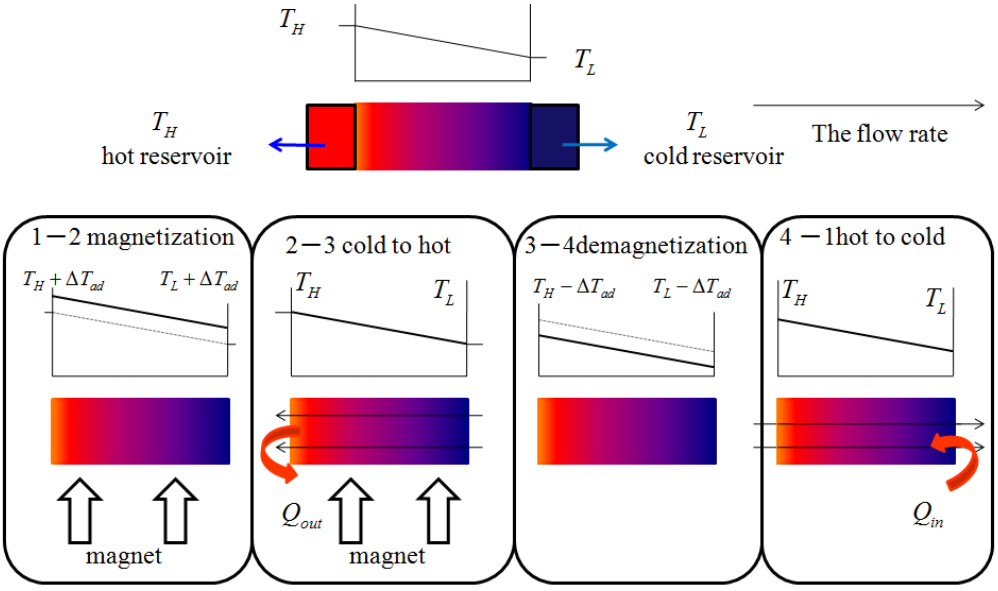

Figure 2-5: AMR cycle

Chapter 3

Modeling AMR

3.1 Two dimension porous media model

In order to deeply understand the physical phenomenon and predict the performance of AMR, a reliable numerical model is required. Until now, the 1-dimentional (1D) numerical model is used in many investigators such as Engelbrecht et al [7]. It based on the determination of the convective heat transfer coefficient between solid and fluid and the friction factor to specify the pressure drop in the fluid due to viscosity. However, considering the unignorable factors in previous studies, heat transfer between the regenerator and outside air in room AMR must be taken account into the practical model. Therefore, we extended the One dimention model to Two dimention model by introducing the convection with air and conduction in y-axis regenerator.

3.1.1 Two dimensional assumption

The model in Figure 3-1 accounts consists of 5 parts, which include the flow of the heat transfer fluid, the MCE of the regenerator material, the heat transfer between the fluid and the solid, the heat transfer between the regenerator and the outside environment, the heat exchange with hot and cold reservoir. The fluid and the solid are incompressible. The properties of the fluid and the solid, such as density, thermal conductivity, viscosity, heat capacity, are constant and evaluated by the initial

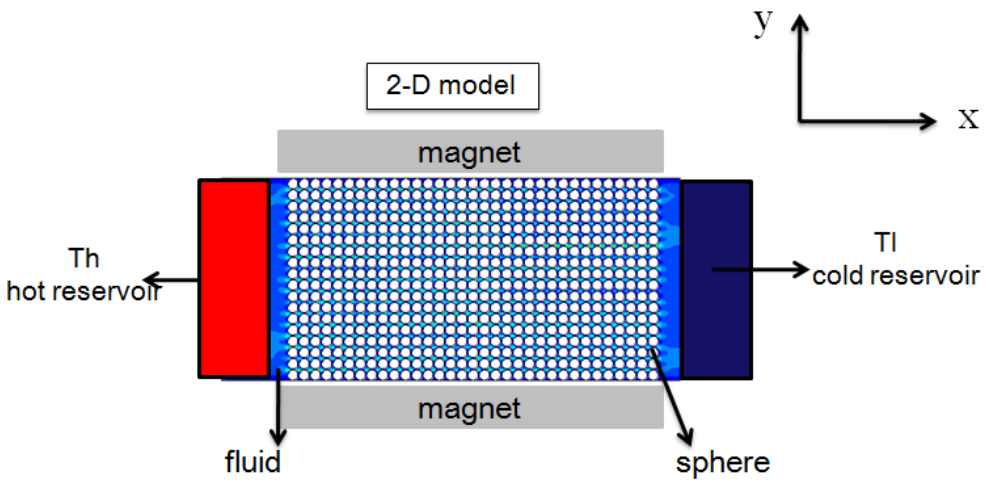

Figure 3-1: Two dimention porous media model of AMR

temperature T_{ini}. The fluid flows in x-axis, and there is a mass flow rate distribution in y-axis. The pressure drop in the fluid is due to viscosity, according to convert the pressure gradient to a friction factor. The friction factor can be evaluated by equation 3.13. The magnetocaloric effect (MCE) is taken into account by the inclusion of a source term in the energy equation for the magnetic solid. A mean field modeling is used to calculate the adiabatic temperature change of the used magnetic material. If dispersion in the regenerator acts to mix the fluid along the bed, then the conduction of fluid can be added to solid and treated as an axial conduction term. The total axial conduction is evaluated by equation 3.8.Axial conduction is taken into account in both x axial and y axial. The heat exchange between the fluid and the reservoir is ideal; the fluid leaves the reservoir and enters the regenerator at the temperature of the associated reservoir. An insulation layer is used to reduce the convective heat transfer between the regenerator and the outside environment, and the convective heat transfer coefficient air is evaluated by equation 3.12.

3.1.2 Governing equations and boundary conditions

The fluid and magnetic material are modeling respectively. The fluid equation and the solid equation are coupled by means of the first convective term, which is the heat

transfer between the fluid and the solid.

$$\begin{aligned} \rho_f C_f \frac{\partial T_f}{\partial t} A_c(y) &= -\dot{m}_f(y,t) C_f \frac{\partial T_f}{\partial x} + h_{eff} A_s A_c(y)(T_r - T_f) + \\ &\quad |\frac{f\dot{m}^3(y,t)}{2\rho_f{}^2 A_c{}^2(y) d_h}| + h_{air} A_c(y^*) \varepsilon (T_f{}^* - T_a ir) \end{aligned} \tag{3.1}$$

$$\begin{aligned} (1-\varepsilon)\rho_r C_r \frac{\partial T_r}{\partial t} A_c(y) &= k_{eff} A_c(y)(1-\varepsilon)\nabla^2 T_f + h_{eff} A_s A_c(y)(T_f - T_r) + \\ &\quad (1-\varepsilon)\rho_r T_r \frac{\partial S}{\partial B}\frac{\partial B}{\partial t} A_c(y) + (1-\varepsilon) h_{air} A_c(y^*)(T_r{}^* - T_{air}) \end{aligned} \tag{3.2}$$

The spatial boundary equations and control equations: Hot to cold($0 < t \leq \tau_1$)

$$\begin{aligned} T_f(x=0,y,t) &= T_h, \\ \frac{\partial T_f}{\partial x}(x=Lx,y,t) &= 0, \\ \frac{\partial T_r}{\partial y}(x,y=0,t) &= 0, \\ \frac{\partial T_r}{\partial y}(x,y=ly,t) &= 0, \\ \dot{m}_f(y,t) &= \dot{m}_f, \\ \frac{\partial S}{\partial B} &= 0. \end{aligned} \tag{3.3}$$

Magnetization($\tau_1 < t \leq \tau_2$)

$$\begin{aligned} \frac{\partial T_f}{\partial x}(x=0,y,t) &= T_h, \\ \frac{\partial T_f}{\partial x}(x=Lx,y,t) &= 0, \\ \frac{\partial T_r}{\partial y}(x,y=0,t) &= 0, \\ \frac{\partial T_r}{\partial y}(x,y=ly,t) &= 0, \\ \dot{m}_f(y,t) &= 0, \\ \frac{\partial S}{\partial B} &= -3.7. \end{aligned} \tag{3.4}$$

Cold to Hot($\tau_2 < t \leq \tau_3$)

$$\begin{aligned} T_f(x = Lx, y, t) &= T_l, \\ \frac{\partial T_f}{\partial x}(x = Lx, y, t) &= 0, \\ \frac{\partial T_r}{\partial y}(x = 0, y, t) &= 0, \\ \frac{\partial T_r}{\partial y}(x, y = ly, t) &= 0, \\ \dot{m}_f(y, t) &= \dot{m}_f, \\ \frac{\partial S}{\partial B} &= 0. \end{aligned} \tag{3.5}$$

Demagnetization($\tau_3 < t \leq \tau_4$)

$$\begin{aligned} \frac{\partial T_f}{\partial x}(x = 0, y, t) &= T_h, \\ \frac{\partial T_f}{\partial x}(x = Lx, y, t) &= 0, \\ \frac{\partial T_r}{\partial y}(x, y = 0, t) &= 0, \\ \frac{\partial T_r}{\partial y}(x, y = ly, t) &= 0, \\ \dot{m}_f(y, t) &= 0, \\ \frac{\partial S}{\partial B} &= 3.7. \end{aligned} \tag{3.6}$$

3.1.3 Reference parameters to the governing equations

Wakao and kague [23]suggest the following empirical correlation for Nusselt number in a packed sphere bed.

$$\begin{aligned} Nu &= 2 + 1.1Re^{0}.6Pr^{\frac{1}{3}}, \\ Re &= \frac{d_h \dot{m}(y,t)}{Ac(y)\mu_f}, \\ Pr &= \frac{C_f}{\mu_f k_f}. \end{aligned} \tag{3.7}$$

The effective thermal conductivity of the solid is evaluated by equation 3.8

$$k_{eff} = k_{static} + k_f D^d \tag{3.8}$$

D^d was suggested by kaviany [13] in equation 3.9

$$D^d = \varepsilon \frac{3}{4} RePr \tag{3.9}$$

$k_{stastic}$, the static conductivity, is evaluated by means of the correlation given by krupiczka (1967).

$$k_{stastic} = k_f \left(\frac{k_r}{k_f} \right)^{0.28 - 0.757 log\varepsilon - 0.057 log \frac{kr}{k_f}} \tag{3.10}$$

The heat transfer coefficient between the fluid and solid has been modified to heff for reducing the entropy generation which will be generated by the temperature difference between the center and the surface of the magnetic material.

$$\begin{aligned} Bi &= \tfrac{d_h h}{k_r}, \\ h &= \tfrac{k_f Nu}{d_h}, \\ h_{eff} &= \tfrac{h}{1+\frac{Bi}{5}}. \end{aligned} \tag{3.11}$$

The heat transfer coefficient between the regenerator and air has been modified to which is evaluated by equation 3.12 [18].

$$h_{air} = \frac{1}{\frac{1}{h_w} + \frac{dx}{k_i}} \tag{3.12}$$

The friction factor of a packed bed of spheres is suggested by Rohsenow (1998) in equation 3.13.

$$f = 300\frac{(1-\varepsilon)^3}{\varepsilon^3 Re} + 3.75\frac{1-\varepsilon}{\varepsilon^3} \tag{3.13}$$

The hydraulic diameter D_h is given by

$$D_h = \frac{2\varepsilon}{3(1-\varepsilon)}dp \tag{3.14}$$

Porosity is ε .Heat transfer surface area A_s (per volume):

$$A_s = 6\frac{1-\varepsilon}{dp} \tag{3.15}$$

The partial B respecting to t in the MCE term can be evaluated by equation 3.14.

$$\frac{\partial B}{\partial t} = \frac{B_{max} - B_{min}}{\tau_2 - \tau_1} \tag{3.16}$$

Table 3.1: The grids used for the simulation

Length of regenerator	Width of regenerator	Cycle time	NXxNYxNT
115mm	15mm	4s	115x30x800

The cooling capacity Qin is evaluated as the ratio between the energy exchanged by the fluid and the cold reservoir during the hot to cold flow and the cycle time, according to equation 3.17.

$$Q_{in} = \frac{1}{\tau}\int_0^{\tau_1} \dot{m}(y,t)C_f(T_f(x=0,y,t) - T_h)dt \tag{3.17}$$

3.1.4 The numerical simulation

The solution of the 2-D model is to provide the temperature filed of both the fluid and the solid. The numerical discretization is based on the Finite Differential Method (FDM) and the temporal integration is marched fully explicit. The enthalpy transfer term, due to the fluid flow is implemented following the up-wind scheme (parankar 1980). This ensures that the thermal energy of the up-wind cell influences the enthalpy transfer term. The initial condition of the fluid and the solid is set to be a linear temperature distribution by forcing a ΔT_{span} between the hot end and the cold end. Table 3.1shows the grids used for the simulation.NX denotes the number of elements in the x-direction and NY denotes the number of elements in the y-direction. An element size is 1mm x 0.5mm.Δt is 5×10^{-3}. The process is completed when the iteration tolerance of T_r and T_f is less than 10^{-3}.

3.1.5 Results and discussion

The cooling capacity of the three kinds of models is compared at the same condition. Only the hot reservoir temperature T_H or the cold reservoir temperature T_L is varied, other parameters are kept constant (see Table 3.2).

The cooling capacity of the 3 kinds of models is compared at the same condition. Only the hot reservoir temperature T_H or the cold reservoir temperature T_L is varied,

Table 3.2: Summary of numerical modeling given parameters

magnetic material	Gd
Fluid	water and ethanol mixture
Total material mass	0.16kg
Regenerator size	$20.312cm^3$
conduction coefficient of the insulation layer	00.19w/mk
Convection coefficient of air	$22w/m^2k$
frequency	0.25
Aspect ratio	7
Mass flow rate	0.0168kg/s
Porosity of matrix	0.356
Thiness of the insulation layer	6mm
Enviroment temperature	292K

other parameters are kept constant. First, T_H is varied from 277K to 313K, and T_L is kept constant at 273K.

Figure 3-2 shows that all of the cooling capacity in 3 models decreases when T_H rises. The trends of change are the same. The difference of the cooling capacity between Q_{in} and Qin_{1D} is caused by the air convection. So the cooling capacity=(Q_{in}-Q_{in1D}) is the air convection loss (CVL). The difference of the $\Delta cooling$ capacity between Q_{in1D} and Q_{in2D} is caused by the conduction of y-axis. So the $\Delta cooling$ capacity =$(Q_{in1D} - Q_{in2D})$is the y-axis conduction loss (CDL). Figure 3-3 shows the percentage of the loss in cooling capacity. When TH rises, both the air convection loss and the conduction loss of y-axis reduce. If the temperature of air is lower than that of fluid, air can help to cooling the fluid instead of resulting loss. This is the reason why the high temperature TH becomes higher, the percentage of the loss in cooling capacity reduces. The conduction loss of y- axis is similar to the air convection loss. The sum of CVL and CDL, i.e.,Tol, can reach to 22% of the cooling capacity, when the TH is 277K and the ΔT_{span} is 4K. When the ΔT_{span} is 40K and T_H is 313K, the total loss decreases down to 12% of the cooling capacity.

Figure 3-4 shows the 3 models with T_L dependence and T_H kept constant at 313K. The cooling capacity increases when T_L rises in 3models.The largest cooling capacity is at T_L =303K in Q_{in2D} model. It is appeared that T_L is higher than environment

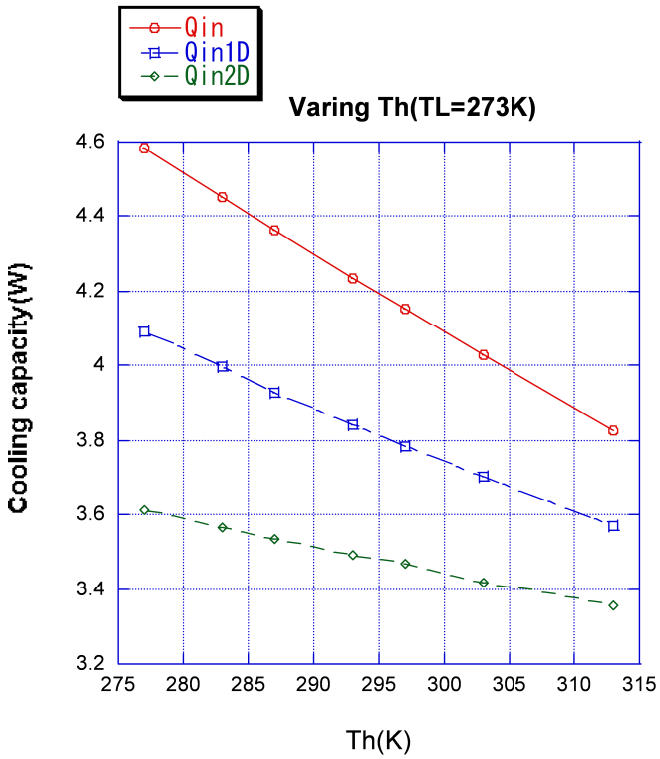

Figure 3-2: Cooling capacity vs T_H (T_H is from 277K to 313K). T_L is 273K. The cycle frequency and the magnetic material mass are kept constant. T_{air} is 292K.Q_{in} is the cooling capacity of 1-D model without considering the air convection. Q_{in1D} is the cooling capacity of 1-D model with considering the air convection. Q_{in2D} is the cooling capacity of 2-D model with considering the air convection and the conduction in y-axis.

Tair, then convection with air can help to reduce the temperature of cold end which will be absorb heat from cold reservoir. When T_L is about 285K, the influence of air convection can be ignorable. This means that when T_H is higher enough and T_L is lower than T_{air}, a proper ΔT_{span} exists in which the influence of air convection can be ignorable. Figure 3-5 shows that the percentage of loss in cooling capacity .The ratio of CVL to total thermal loss and CDLs is roughly the same. When the low temperature T_L becomes higher and higher, even over the air temperature, air can help to cooling the fluid. At this time, the percentage of loss will be minus. After comparing the 3 kinds of model, what is known is that the influence of air convection and conduction of y axial is not small enough to be ignored. Moreover, the calculation time of the 2-D model is less than 10 minutes. It is reasonable to analyze

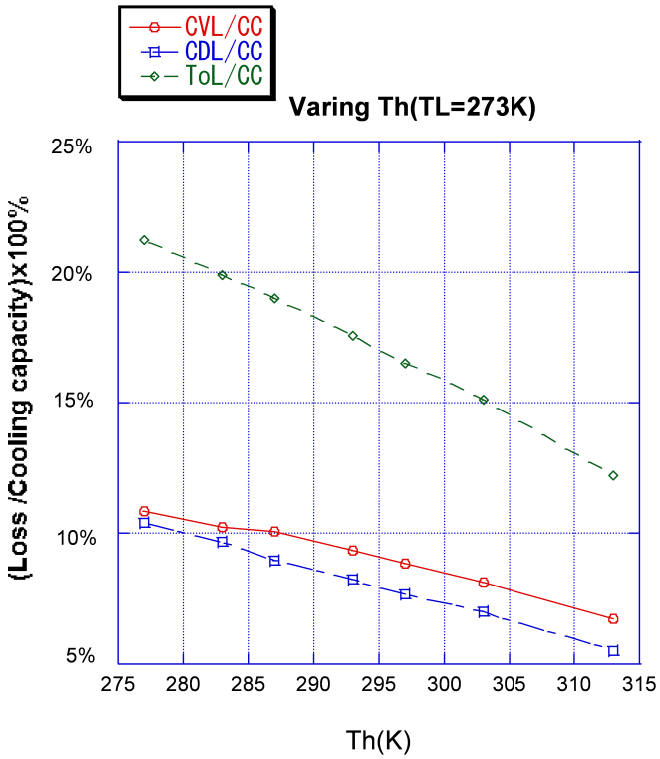

Figure 3-3: The percentage of loss in cooling capacity (CC) vs T_H. T_L is 273K. TH is varied from 274K to 313K. T_{air} is 292K. There are 3 kinds of loss, convection loss (CVL), conduction loss of y axial (CDL), and the sum of convection loss and conduction loss of y axial (Tol).

many different configurations and operating conditions. So the Q_{in2D} model would be proper to predicting the performance of room AMR considering the ignorable factor in practice.

3.1.6 Conclusions

A time independent, 2-dimension porous media model was developed for predicting the room AMRR. The 2-D model and the previous 1-D model were compared. It is concluded that the system can lose 22% of cooling capacity caused by air con-vection and the conduction loss in y-axis. The ratio between convection loss and conduction loss was roughly same. Thus, our 2-D model will predict the room AMR for including the influence of air convection and conduction of y-axis.

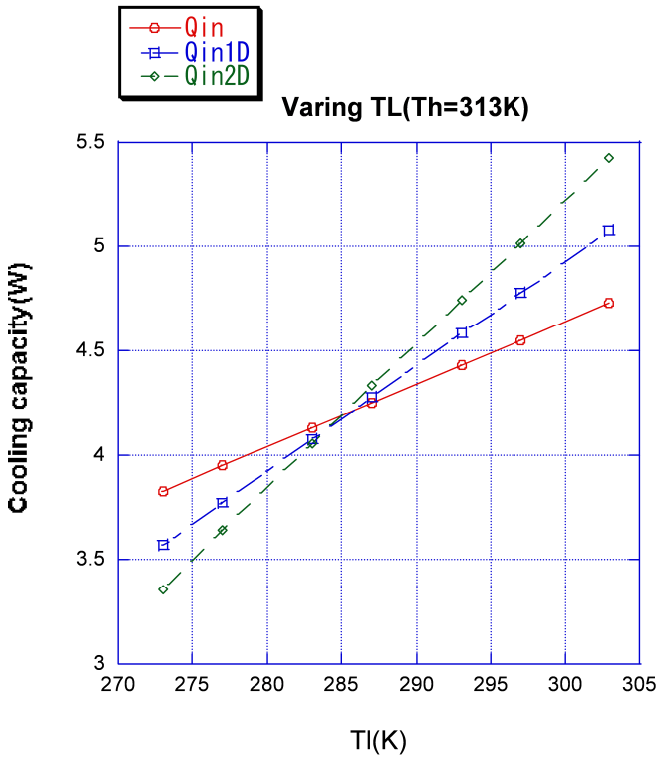

Figure 3-4: Cooling capacity vs T_L (T_L is from 273K to 303K). T_H is 313K. T_{air} is 292K.

3.2 Investigation of Two dimension porous media and flat plate models by FVM

The results generated by the 1-D model, although valuable, show discrepancies with experimental data, but the differences are mainly caused by the use of the heat transfer correlation. To eliminate the use of heat transfer and pressure drop correlations, the velocity, pressure and tem- perature field must to be solved simultaneously. In doing so, a 2-dimension porous media model close to reality has been modeled. The 2-D model is based on the two-dimensional Navier-Stokes equations for the fluid flow around the discrete particles which are alternatively heated and cooled during magnetization and demagnetization. The adopted numerical solution is explained and typical results are presented and analyzed.

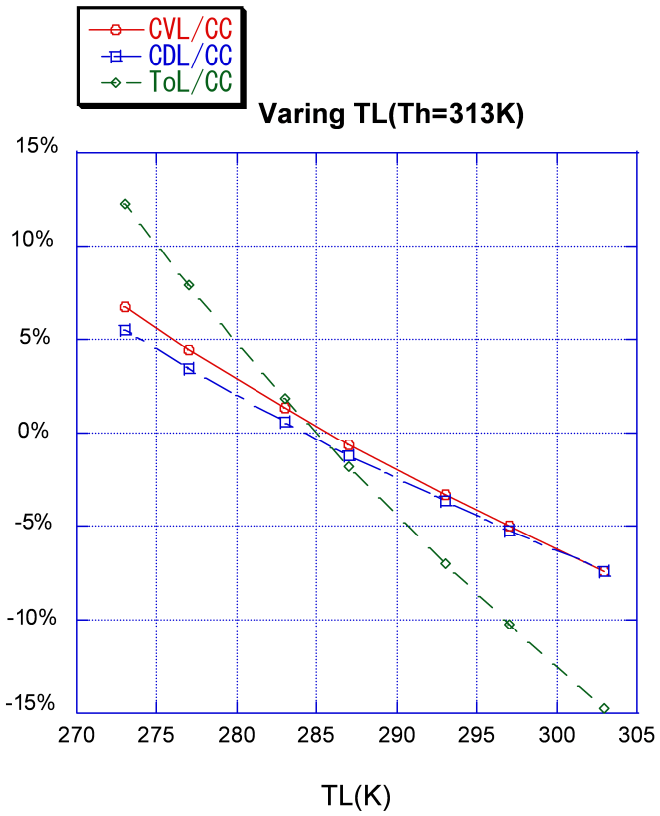

Figure 3-5: The percentage of loss in cooling capacity vs TL. TL is from 273K to 303K .TH is 313K.Tair is 292K.

3.2.1 Governing Equations and boundary condition

Two dimensional incompressible N-S equations based on laminar assumption.

Fluid zone

Continuum Equation:

$$\frac{\partial \mu}{\partial x} + \frac{\partial \nu}{\partial y} = 0 \tag{3.18}$$

Momentum equation:

$$\frac{\partial u}{\partial t} + u\frac{\partial u}{\partial x} + \nu\frac{\partial u}{\partial y} = -\frac{1}{\rho_f}\frac{\partial p}{\partial x} + \mu \left(\frac{\partial^2 u}{\partial x^2} + \frac{\partial^2 u}{\partial y^2} \right) \tag{3.19}$$

Energy equation:

$$\frac{\partial T_f}{\partial t} + u\frac{\partial T_f}{\partial x} + \nu\frac{\partial T_f}{\partial y} = k \left(\frac{\partial^2 T_f}{\partial x^2} + \frac{\partial^2 T_f}{\partial y^2} \right) \tag{3.20}$$

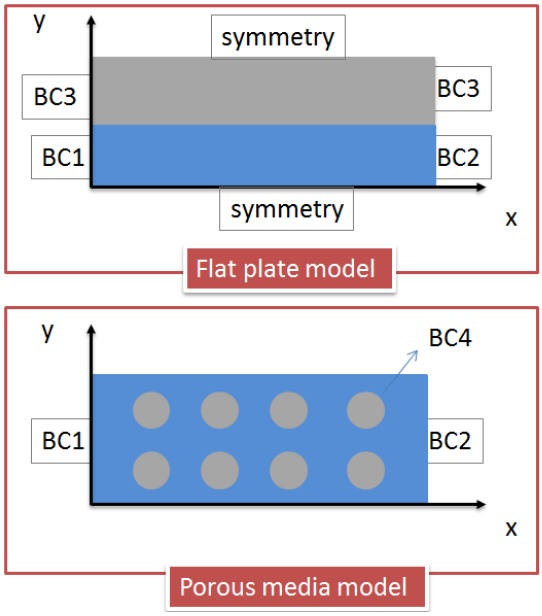

BC1: Inlet velocity and static temperature

BC2: Zero gradient

BC3: Adiabatic conditions

BC4: Coupled wall(heat flux and temperature)

Symmetry: No-slide and adiabatic

Figure 3-6: 2-D model boundary conditions

u, ν, p and T_f are basic values for solution, which mean velocity components, pressure and temperature of the fluid.

Solid Zone

Energy equation:

$$\rho_s C_p \frac{\partial T_r}{\partial t} = k \left(\frac{\partial^2 T_f}{\partial x^2} + \frac{\partial^2 T_f}{\partial y^2} \right) + S_t \tag{3.21}$$

$T_r$is the temperature in the solid zone, S is the source term, in this research, it can be used to demonstrate the magnetic effect. Figure 3-6 shows the boundary conditions.

3.2.2 Numerical Method

The finite volume method(FVM) is used in this research, and the solid and fluid zone are discretized by using triangular unstructured mesh respectively(in Figure 3-7). The schemetic of discretization is showed in Table 3.2. In the fluid zone, the variable separation solver is adopted, in which the pressure is uncoupled with velocity by using SIMPLEC method(Semi-Implicit Pressure Linked Equation Consistent), firstly, the

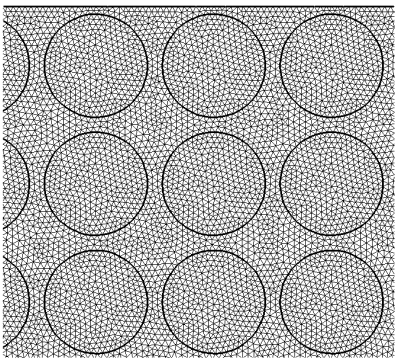

Figure 3-7: Schemetic of mesh

Table 3.3: The scheme for discretization

Pressure	Second-order central scheme
Convective term in fluid zone	Second-order central scheme
Diffusion term in fluid and solid zone	Second-order central scheme
Unsteady term	Second-order central scheme

momentum equations are solved in the cell-based grid, then the pressure field is corrected by using pressure-correction equation, which is educed from continuum equation, and the velocity components are corrected by using pressure correction value, after that, the energy equation are solved to obtain temperature. In the solid zone, the heat conductive equation is solved, and the source term is activated, when the magnetic field is acting:

$$S_t = \frac{\rho_s C_p \Delta T_s(H, T_c)}{\delta t} \tag{3.22}$$

3.2.3 Results and discussion

In order to optimize AMR applications, we considered the same conditions that the AMR device developed in the laboratory and varied the model inputs, velocity and frequency, especially modeling the influence of velocity to the heat transfer rate from practical to fluid and pressure loss.Table 3.4shows the reference numerical parameters which are used in the simulation. Figure 3-8 shows the temperature field for the heat

Table 3.4: Reference values of the numerical parameters

magnetic material	Gd
Fluid	water and ethanol mixture
Total material mass	0.16kg
Regenerator size	$20.312cm^3$
Mean particle size	$50\mu m$
Porosity of matrix	0.356
B_{max}	1.2T
B_{min}	0T
ΔT_s	2K
T_H	313K
T_L	293K

transfer course under different Inlet velocity. After magnetizing, the fluid flow from cold end to hot end (in the graph is from left to right). We found that heat transfer in high Inlet velocity (0.025m/s) is already in stable state at stable state at 0.3 second, while the heat transfer in low Inlet velocity (0.005m/s) still in an unstable state. It implies that high velocity can fast heat transfer. Figure 3-9 and Figure 3-10 shows the velocity field while the inlet velocity is 0.001m/s. The fastest x- velocity appears in the gap between the particles and can be 10 times of the inlet velocity in Figure 3-9. The y-velocity can be minus for the reverse circulation flow rate in Figure 3-10.

The velocity is changed from 0.007m/s to 0.025m/s and the results are shown in Figure 3-12. Figure 3-12 left is the heat transfer rate from particle to fluid. It is observed that a higher velocity results in a higher heat transfer rate. Figure 3-12 right illustrates the pressure loss. The pressure loss has a positive correlation to the velocity, which is similar to the heat transfer rate. Since a higher velocity will result in a higher transfer rate as well as a higher pressure loss, an optimized velocity can be found for the best energy efficiency.

Figure 3-11 shows the correlation of velocity and COP, cooling capacity. When the frequency is 0.25 and the velocity is from 0.006m/s to 0.014m/s, the COP has a peak value near 6.94 for COP and cooling capacity with respect to operation frequency. When the frequency is varied from 0.25 to 1.45 Hz, the COP has a peak value near

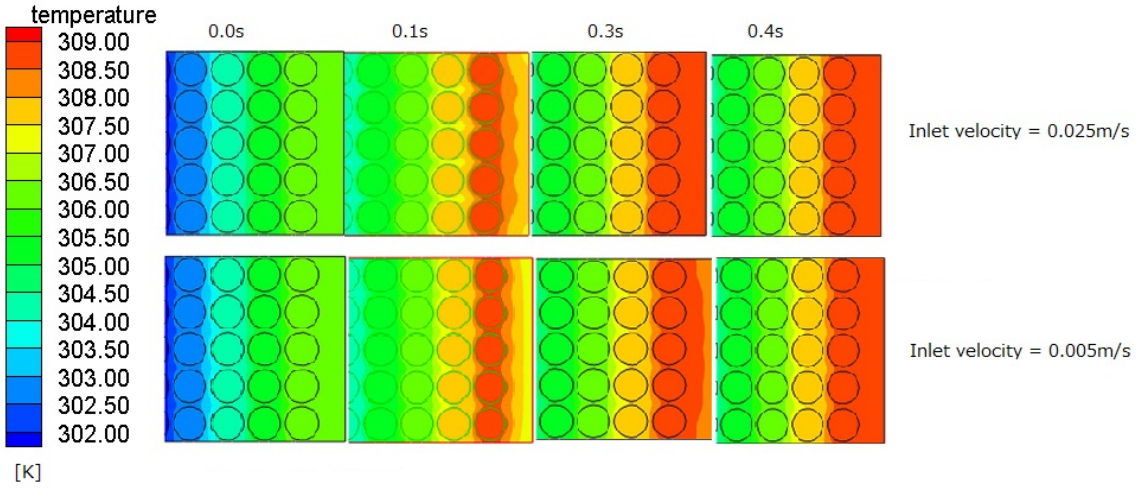

Figure 3-8: Temperature field for the heat transfer course under different Inlet velocity.

7.4. The cooling capacity increases quickly when the operation frequency is higher. A high operation frequency is required for the high cooling capacity.

After comparison, we found that high velocity can make the heat transfer rate higher for the different regenerator geometries (Figure 3-11). So a high operation frequency is needed to improve the cooling capacity. In the high velocity field, the flat plate model is better than the porous media model for the improved pressure drop (Figure 3-13), which means improvement in the COP of AMR can be expected.

3.2.4 Conclusions

A transient 2-dimensional porous media model of a reciprocating AMR has been constructed and solved numerically. The coupled effects of the temperature and velocity fields have been taken into account. The magneto-caloric effect is also taken into account by the inclusion of a source term in the energy equation for magnetic solid. The fluid flow through the interstitial channels formed by the magnetic particles is modeled by the two dimensional incompressible N-S equations based on laminar assumption. In particular, detailed model results regarding heat transfer and pressure drop show that an optimized velocity can be found for the energy efficiency. The effect of changing the operating cycle frequency shows that there is a maximum COP for a

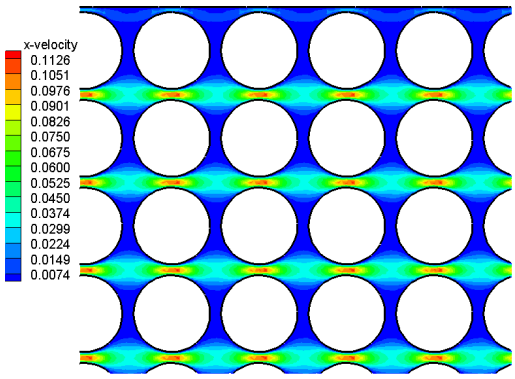

Figure 3-9: X-velocity field. Inlet velocity is 0.001m/s.

given T span. A high operation frequency is required for a high cooling capacity.

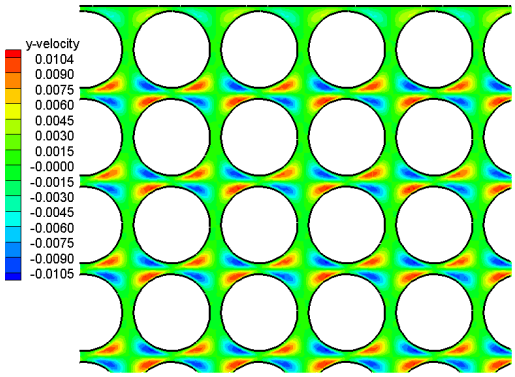

Figure 3-10: Y-velocity field. Inlet velocity is 0.001m/s.

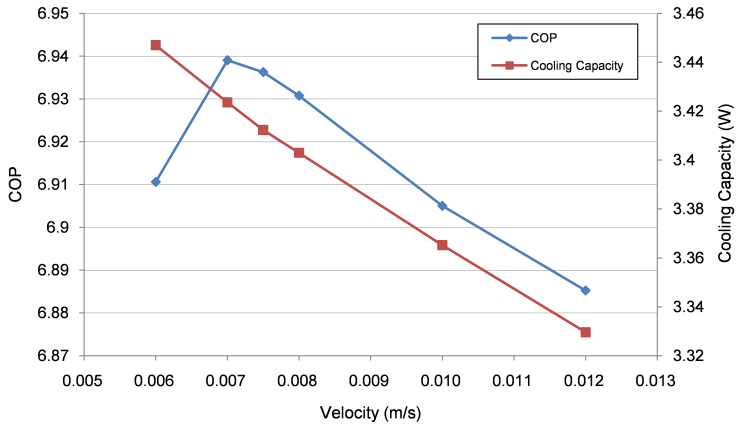

Figure 3-11: Velocity vs COP and cooling capacity.

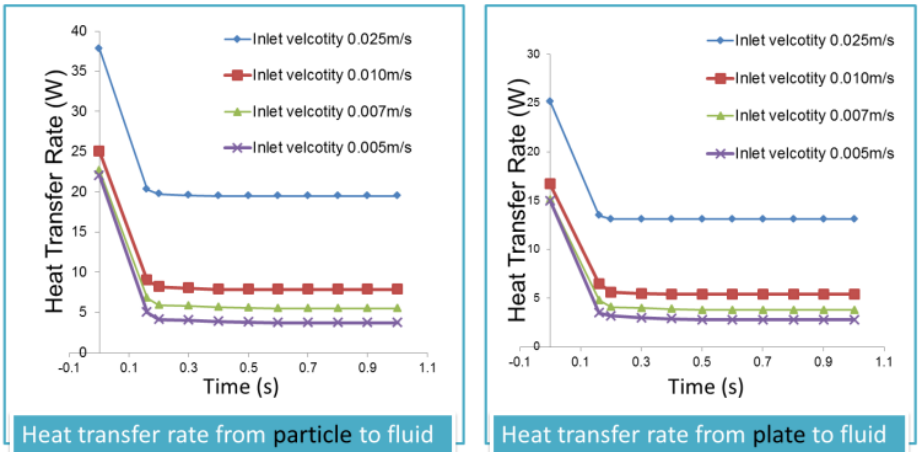

Figure 3-12: Comparison of heat transfer rate in 2 kinds of models.

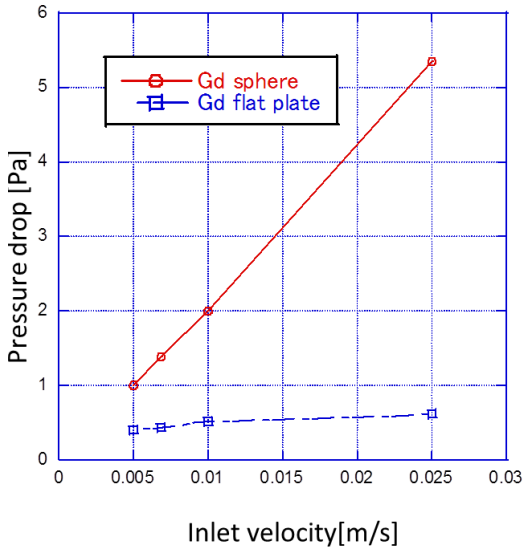

Figure 3-13: Comparison of pressure drop result in 2 different kinds of models.

Chapter 4

Optimization of regenerator by Geometry design

4.1 Introduction of regenerator

Regenerator is not just a material container where magnetic material generates and absorbs heat, but also a flow path. Figure 4-1 left showed the typical one stage compressor refrigeration system. After replacing the compressor, we can get a schematic of AMR system. In AMR system, there are four key parts: regenerator, motor, magnet, cold and heat exchanger. The most important part is regenerator. Figure 4-2 shows one type of regenerator, packed sphere regenerator. Inside the regenerator, heat transfer fluid change heat with magnetic material and then flow out changing heat with outside environment. The mechanical losses, due to pressure drop, axes conductivity, heat transfer between material and fluid, happen inside it. To improve the performance of AMR system, regenerator should be enhanced to let the heat generated by magnetic material be used as efficient as possible.

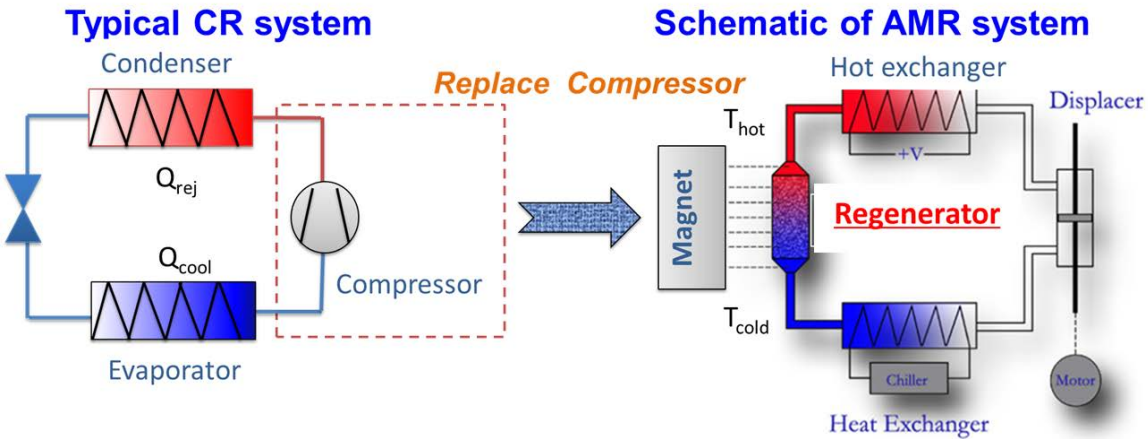

Figure 4-1: Left is a one stage typical compressor refrigeration system. Right is a schematic of AMR system.

Figure 4-2: Left is a one stage typical compressor refrigeration system. Right is a schematic of AMR system.

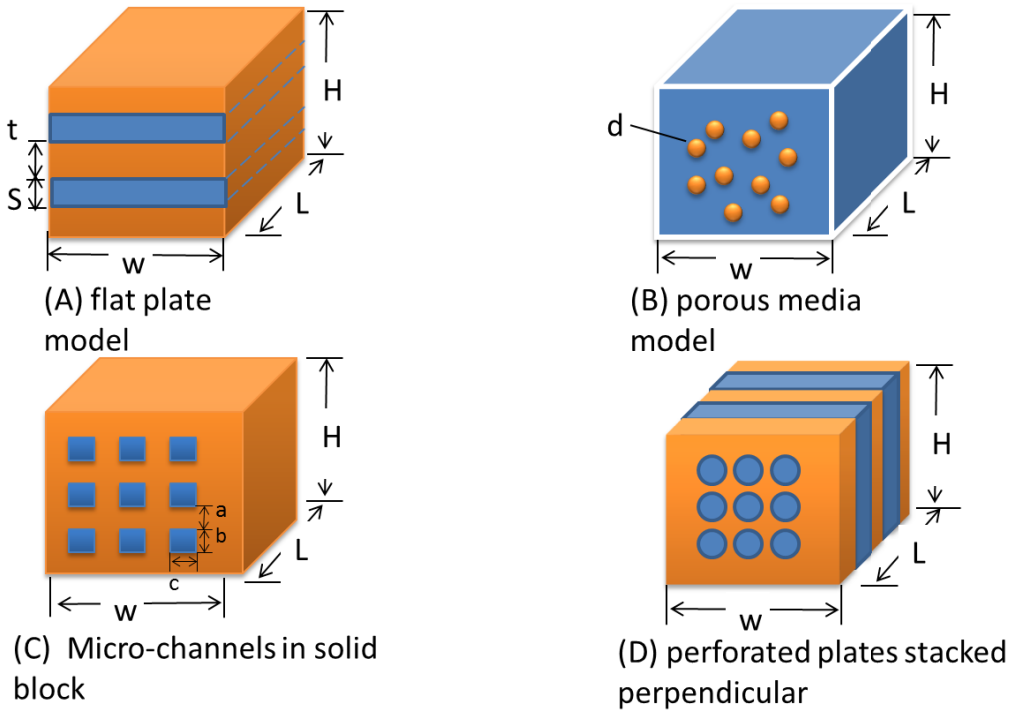

Figure 4-3: Potential geometry design.

4.1.1 Potential regenerators

4.2 Motivation

To commercialize MR technology, two major regenerator optimization methods have been considered. One is to utilize the multi-layered regenerator, which can realize a big MCE over a wide temperature span by layering several magnetic materials carefully on top of the regenerator. Another method is to improve the geometry design of the regenerator. So far the choices of geometry have been limited to flat plate and packed sphere design, and few papers focus on discussion of geometry design either from theoretical or experimental perspectives. Barclay(1984) [1] used a simple algorithm to simulate and compare Four types of regenerator which is showed in Figure 4-3[1]. Besides the aforementioned two popular designs, he also suggested microchannel and perforated plate stack geometries can be candidates to reduce the longitudinal conduction loss in the bed. However, the accuracy of the numerical results is limited by the simplicity of the simulation. Recently, K.Engelbrecht et al.(2010) also

did experimental and numerical studies on passive regenerator geometries [8]. They tested 18 aluminum plates, including flat plate, corrugated plate and dimpled plate regenerators, and determined the optimum type of plates regenerator has 0.2 mm-0.3 mm plate thickness. Tura compared packed sphere and micro-channel regenerator experimentally and suggested spheres act as a more effective regenerator [21]. Jaka-Tusek(2013) experimentally analyzed both parallel-plate and packed sphere AMRs and concluded that parallel-plate AMRs provide the most efficient heat transfer and other types of ordered structures with non-uniform porosity decreases [22]. However, comparison and numerical analysis of the parallel-plate, packed sphere and micro-channel regenerators has not been discussed yet. The goal of this chapter is to compare and discuss the details of heat process in three regenerators numerically.

4.3 Governing equations and boundary conditions

One dimentional AMR models have been constructed. The models like other All numerical models of the AMR are based on a mathematical model describing heat transfer in a solid matrix structure, the MCE in the solid due to the changing magnetic field, and the coupling to the convective heat transfer of a fluid. The fluid and magnetic material are modeling respectively.MCE is taken into account by the inclusion of a source term in the energy equation for the magnetic solid. A mean field modeling is used to calculate the adiabatic temperature change of the used magnetic material. Dispersion in the regenerator acts to mix the fluid along the bed, and the conduction of fluid can be added to solid and treated as an axial conduction term. The heat exchange between the fluid and the reservoir is ideal; the fluid leaves the reservoir and enters the regenerator at the temperature of the associated reservoir. The properties of the fluid and the solid, such as density, thermal conductivity, viscosity, heat capacity, are constant and evaluated by the initial temperature T_{ini}.The

governing equations and boundary conditions are given as follow:

$$\begin{aligned} \rho_f C_f \frac{\partial T_f}{\partial t} A_c(y) &= -\dot{m}_f(y,t) C_f \frac{\partial T_f}{\partial x} + h_{eff} A_s A_c(y)(T_r - T_f) + \\ &\quad |\frac{f\dot{m}^3(y,t)}{2\rho_f{}^2 A_c{}^2 d_h}| \end{aligned} \tag{4.1}$$

$$\begin{aligned} (1-\varepsilon)\rho_r C_r \frac{\partial T_r}{\partial t} A_c &= k_{eff} A_c (1-\varepsilon)\nabla^2 T_f + h_{eff} A_s A_c (T_f - T_r) + \\ &\quad (1-\varepsilon)\rho_r T_r \frac{\partial S}{\partial B}\frac{\partial B}{\partial t} A_c \end{aligned} \tag{4.2}$$

Hot to cold

$$\begin{aligned} T_f(x=0) &= T_h, \\ \frac{\partial T_f}{\partial x}(x=Lx) &= 0 \end{aligned} \tag{4.3}$$

Cold to Hot

$$\begin{aligned} T_f(x=Lx) &= T_l, \\ \frac{\partial T_f}{\partial x}(x=0) &= 0 \end{aligned} \tag{4.4}$$

The three models,packed sphere,flat plate and micro-channel regenerator, have the same governing equations and boundary conditions. However part of the reference parameters are different in equations.

4.4 Parameters in modeling

Main parameters in packed sphere regenerator

Main parameters in packed sphere regenerator are showed in Chapter 3.1.3.

Main parameters in flat plate regenerator

The hydraulic diameter D_h is given by

$$D_h = \frac{\varepsilon}{1-\varepsilon} dp \tag{4.5}$$

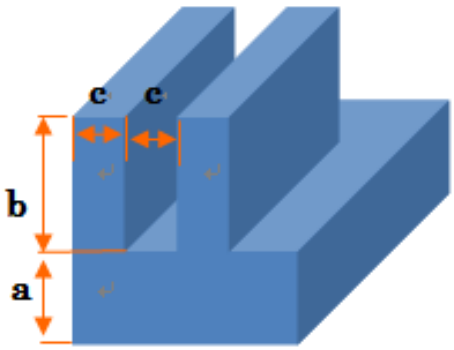

Figure 4-4: Schametic of Micro-channel regenerator.

For more turbulent-like fluid flow, the Nusselt number (Nu) is suggested by Tura[3]which is defined by Reynolds Number (Re):

$$Nu = 8.235 \tag{4.6}$$

For Laminar flow, the friction factor is given by

$$f = \frac{64}{Re} \tag{4.7}$$

Porosity is ε .Heat transfer surface area As (per volume):

$$A_s = 2\frac{1-\varepsilon}{dp} \tag{4.8}$$

Main parameters in Micro-channel regenerator

The shchameic of Micro-channel regenerator is showed in Figure 4-4 The hydraulic diameter D_h is given by

$$D_h = \frac{2cb}{c+b} \tag{4.9}$$

For more turbulent-like fluid flow, the Nusselt number (Nu) is suggested by Tura[3]which is defined by Reynolds Number (Re):

$$Nu = 0.48 + 0.18Re^{1}.3 \tag{4.10}$$

For Laminar flow, the friction factor is given by

$$f = \frac{16}{Re} \tag{4.11}$$

Porosity is ε .Heat transfer surface area As (per volume):

$$A_s = \frac{2(b+c)}{(2a+bc)}(1-\varepsilon) \tag{4.12}$$

Correlation between b and a:

$$b = \frac{2\varepsilon}{1-2\varepsilon}a \tag{4.13}$$

To help define the effect of the aspect ratio, Z has been defined as:

$$z = \frac{min(b,c)}{max(b,c)} \tag{4.14}$$

According to the XF Peng (1996) [15], the experiments demonstrated the laminar friction factor or flow resistance reaches a minimum value as z is 0.5.

The common parameters are as follow: Number of Transfer Unites (NTU) is:

$$NTU = \frac{h_{eff}A_s}{\dot{m}C_f} \tag{4.15}$$

Figure of Merit (FOM) is defined by the rejection heat Q_{out}, refrigeration load Q_{in} and power required :

$$FOM = \frac{Q_{out} - Q_{in}}{\dot{w} + (Q_{out} - Q_{in})} \tag{4.16}$$

4.5 Entropy generation minimization

Entropy generation minimization (EGM) is also known as thermodynamic optimization in engineering. It is the method of optimization of real devices and processes based on the most basic concepts of heat transfer, fluid mechanics and thermodynamics. In AMR systems, the irreversibility related to: heat and fluid flow in regenerator; pump inefficiency; the magnetization system; the process of magnetization and var-

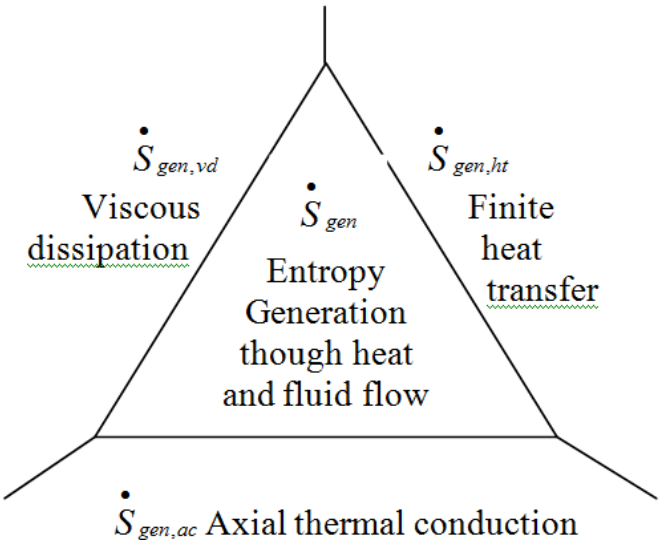

Figure 4-5: Schametic of EGM.

ious heat leaks. Heat transfer between the fluid and the magnetocaloric material is the major loss mechanism in AMR systems. In order to maximize AMR performance, it is critical to understand heat transfer processes and minimize the entropy generation though heat and fluid flow in the regenerator. In this paper, we use the EGM method to optimize the regenerator design. The total entropy generation $\dot{S}_{gen}$, which is due to irreversible processes though heat and fluid flow in the regenerator, can be considered in 3 parts (Figure 4-5) [1].

The total entropy generation $\dot{S}_{gen}$ is the sum of the three items:

$$\dot{S}_{gen} = \dot{S}_{gen,ht} + \dot{S}_{gen,vd} + \dot{S}_{gen,ac} \tag{4.17}$$

The entropy generation due to finite heat transfer between the heat transfer fluid and magnetic material $\dot{S}_{gen,ht}$ is:

$$\dot{S}_{gen,ht} = \frac{Q_R}{Ntu+1}\left(\frac{1}{T_{cold}} - \frac{1}{T_{hot}}\right) \tag{4.18}$$

where

$$Q_R = \dot{m}_f C_p (T_h - T_c) \tag{4.19}$$

The entropy generation due to viscous dissipation of the flow energy $\dot{S}_{gen,ac}$ is:

$$\dot{S}_{gen,ac} = \frac{K_{eff} A_c}{L} \frac{(T_{hot} - T_{cold})^2}{T_{cold} T_{hot}} \tag{4.20}$$

The entropy generation due to axial thermal conductivity of the regenerator material $\dot{S}_{gen,vd}$ is:

$$\dot{S}_{gen,vd} = \frac{V_f \Delta P}{T_{hot}} \tag{4.21}$$

The required work $\dot{W}$ is:

$$\dot{W} = (Q_{out} - Q_{in}) + T_h \dot{S}_{gen} \tag{4.22}$$

The coefficient of performance COP can be caculated as:

$$COP = \frac{Q_{in}}{\dot{W}} \tag{4.23}$$

4.6 Comparison of packed sphere and flat plate regenerator

4.6.1 Results and discussion

Table 4.1 summarizes the given parameters. At lower frequencies the cooling capacity will be lower, and at higher frequencies eddy current and hysteresis losses generate heat in the regenerator. Consider the situation above, 0.25, 0.5, 1.0 Hz have been chosen based on the experimental AMRs for comparing 2 models. Since the material mass is kept constant, increased porosity will result in increased regenerator volume, requiring a large magnet. A randomly porosity 0.365 which is used in experimental AMR, is fixed. The aspect ratio is limited in 2, 7, 14 for 2 models. Figure 4-6, 4-7, 4-8 shows the entropy generation corresponding to the different plate thickness at frequency 0.25Hz, 0.5Hz, 1Hz in the flat plate model. It is observed that increased plate thickness increases entropy generation especially in high frequency. We can get

Table 4.1: Reference values of the numerical parameters

magnetic material	Gd	frequency	0.25, 0.5, 1
Fluid	water and ethanol mixture	Aspect ratio	2,7,14
Total material mass	0.16kg	particle size	$100 - 800\mu m$
Regenerator size	$20.312cm^3$	Porosity of matrix	0.356
B_{max}	1.2T	Plate thickness	$60 - 700\mu m$
B_{min}	0T	ΔT_s	2K
T_H	307K	T_L	277K

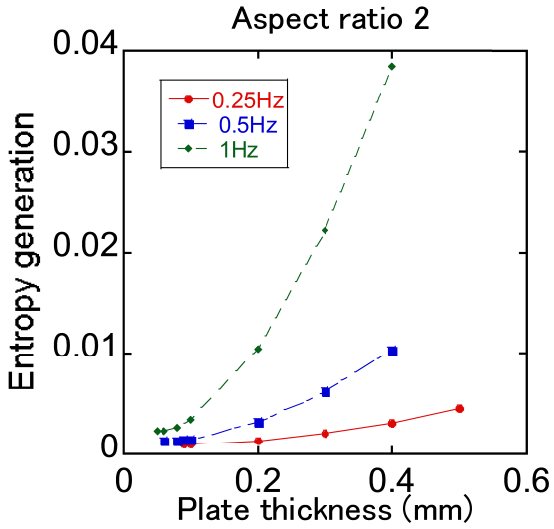

Figure 4-6: Entropy generation corresponding to the different plate thickness at frequency 0.25Hz, 0.5Hz, 1Hz and ascpet ratio 2 in the flat plate model.

the minimization entropy generation around 0.1mm. High frequency can result in a high entropy generation, but when the Aspect ratio is 14, the difference entropy generation in difference frequency is very small. It is also can be seen in Figure 4-9, 4-10, 4-11 which shows the entropy generation corresponding to the different sphere size at frequency 0.25Hz, 0.5Hz, 1Hz in the porous media model.The minimization entropy generation can be achieved around 0.3mm sphere size, frequency 0.25Hz, aspect ratio 14. Figure 4-12,4-13,4-14,4-15,4-16 and 4-17 showed the cooling capacity in two models.Figure 4-18,4-19, 4-20, 4-21,4-22 and 4-23 showed the coefficient

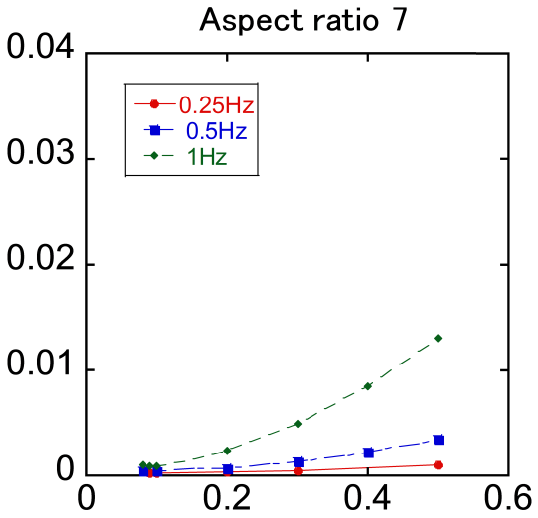

Figure 4-7: Entropy generation corresponding to the different plate thickness at frequency 0.25Hz, 0.5Hz, 1Hz and ascpet ratio 7 in the flat plate model.

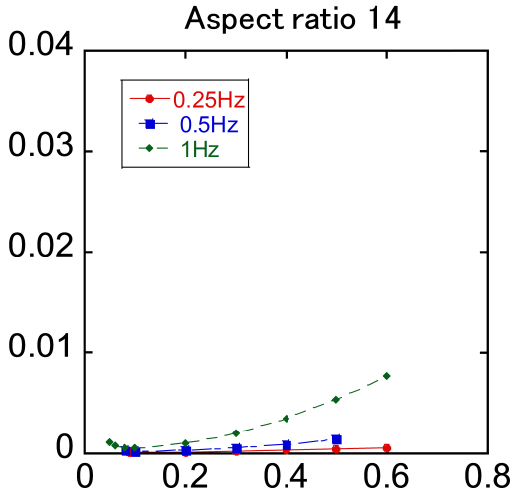

Figure 4-8: Entropy generation corresponding to the different plate thickness at frequency 0.25Hz, 0.5Hz, 1Hz and ascpet ratio 14 in the flat plate model.

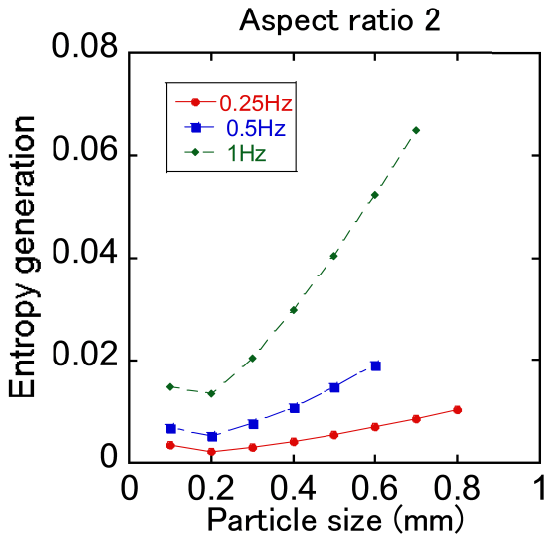

Figure 4-9: Entropy generation corresponding to the different particle size at frequency 0.25Hz, 0.5Hz, 1Hz and ascpet ratio 2 in the porous media model.

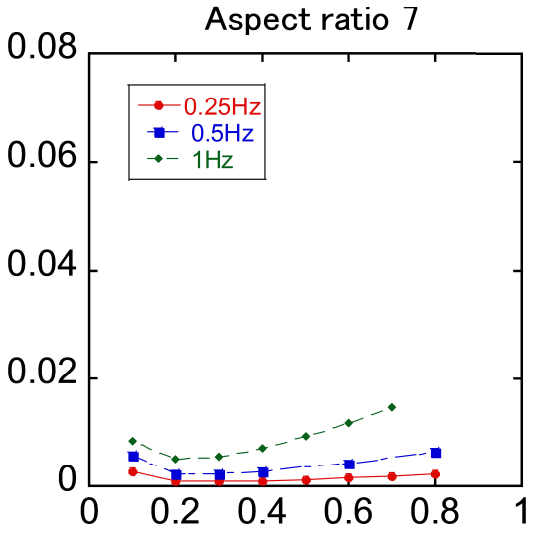

Figure 4-10: Entropy generation corresponding to the different particle size at frequency 0.25Hz, 0.5Hz, 1Hz and ascpet ratio 7 in the porous media model.

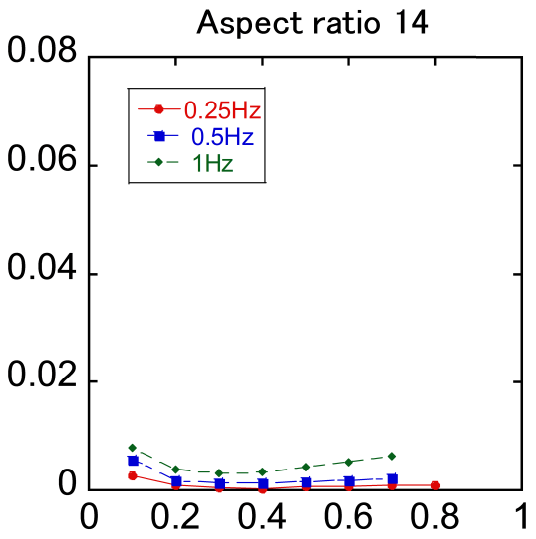

Figure 4-11: Entropy generation corresponding to the different particle size at frequency 0.25Hz, 0.5Hz, 1Hz and ascpet ratio 14 in the porous media model.

of performance (COP) in two models. In the figures, increased frequency can get an increased cooling capacity and small aspect ratio can get more cooling capacity for the more mass flow rate which is resulted by bigger across surface. The biggest cooling capacity of flat plate model is bigger than that of porous media model. An optimized flat plate thickness and sphere size can be found for the best COP. The optimized thickness is almost the same under different frequency. It is also found that COP decrease but cooling capacity significantly increase for the increased frequency both in flat plate model and porous media model. Decreased COP can be explained by the figures which are showing the entropy generation of the models. Increased frequency will increase the total entropy generation. When the thickness is bigger than optimized point, increased thickness will significant increase the heat transfer generation entropy for the decreased heat transfer surface. In porous media model, the optimized sphere size will be around 0.2mm to 0.3mm. On the other hand, 0.1mm to 0.2mm thickness plate will be more efficient. Comparing the two models, flat plate model can get a smaller entropy generation and achieve a higher cooling capacity.

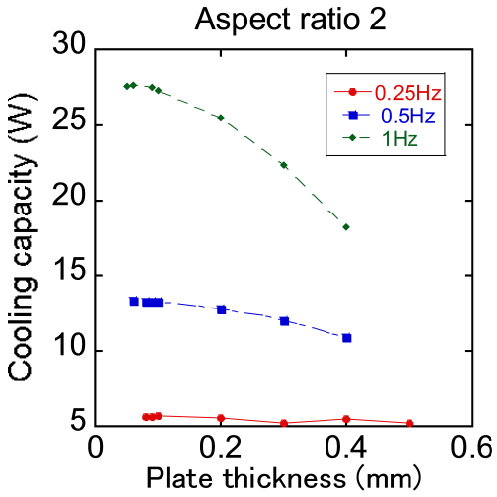

Figure 4-12: Cooling capacity corresponding to the different plate thickness at frequency 0.25Hz, 0.5Hz, 1Hz and ascpet ratio 2 in the flat plate model.

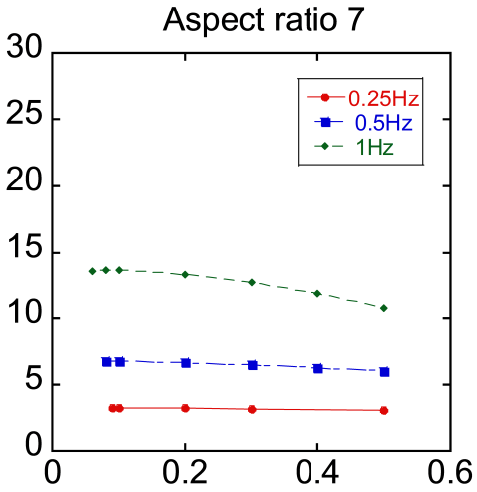

Figure 4-13: Cooling capacity corresponding to the different plate thickness at frequency 0.25Hz, 0.5Hz, 1Hz and ascpet ratio 7 in the flat plate model.

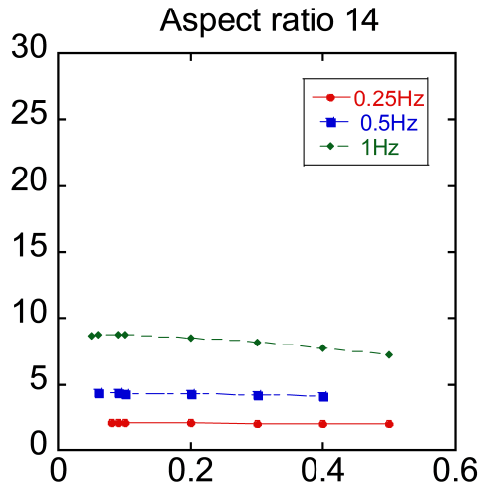

Figure 4-14: Cooling capacity corresponding to the different plate thickness at frequency 0.25Hz, 0.5Hz, 1Hz and ascpet ratio 14 in the flat plate model.

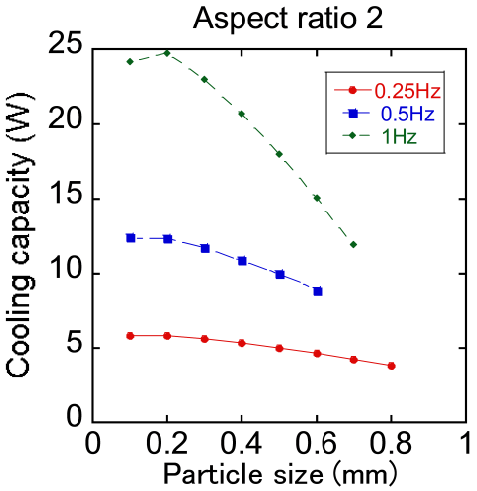

Figure 4-15: Cooling capacity corresponding to the different particle size at frequency 0.25Hz, 0.5Hz, 1Hz and ascpet ratio 2 in the porous media model.

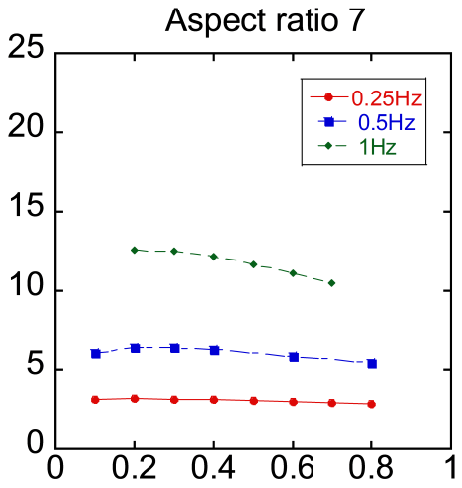

Figure 4-16: Cooling capacity corresponding to the different particle size at frequency 0.25Hz, 0.5Hz, 1Hz and ascpet ratio 7 in the porous media model.

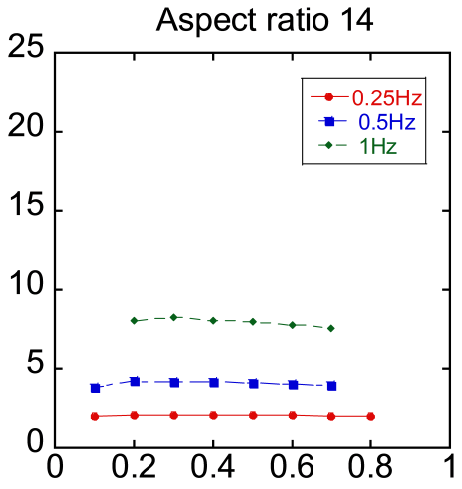

Figure 4-17: Cooling capacity corresponding to the different particle size at frequency 0.25Hz, 0.5Hz, 1Hz and ascpet ratio 14 in the porous media model.

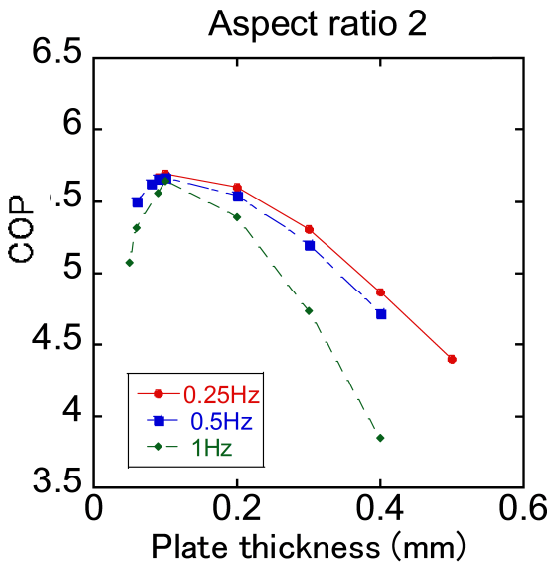

Figure 4-18: COP corresponding to the different plate thickness at frequency 0.25Hz, 0.5Hz, 1Hz and ascpet ratio 2 in the flat plate model.

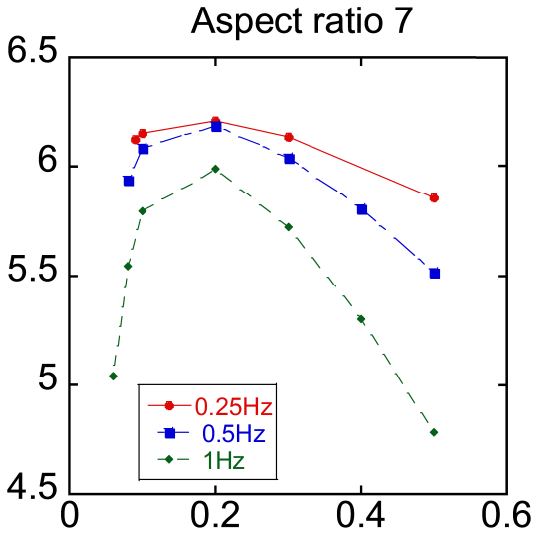

Figure 4-19: COP corresponding to the different plate thickness at frequency 0.25Hz, 0.5Hz, 1Hz and ascpet ratio 7 in the flat plate model.

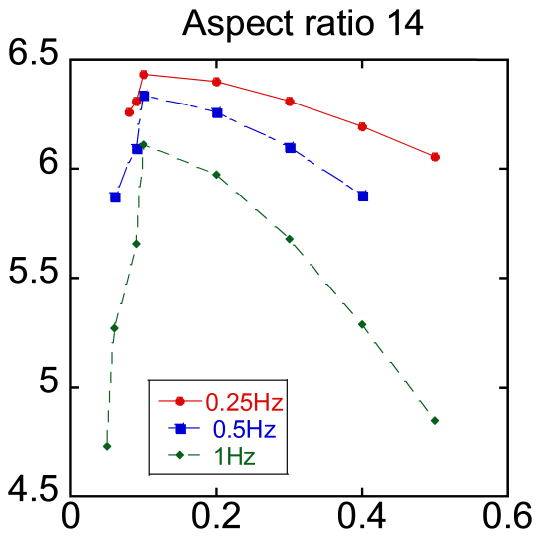

Figure 4-20: COP corresponding to the different plate thickness at frequency 0.25Hz, 0.5Hz, 1Hz and ascpet ratio 14 in the flat plate model.

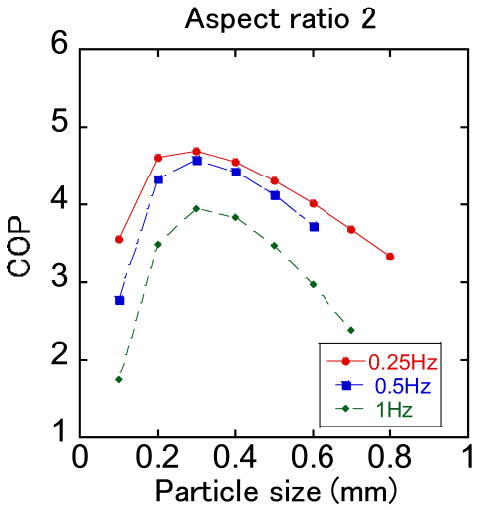

Figure 4-21: COP corresponding to the different particle size at frequency 0.25Hz, 0.5Hz, 1Hz and ascpet ratio 2 in the porous media model.

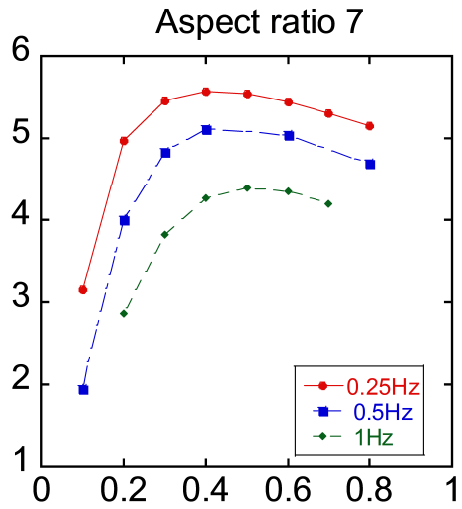

Figure 4-22: COP corresponding to the different particle size at frequency 0.25Hz, 0.5Hz, 1Hz and ascpet ratio 7 in the porous media model.

4.6.2 Conclusions

Since the heat transfer mechanism in the AMR is same as that in the ordinary thermal regenerator except for the steps of application and removal magnet, EGM which is widely used in heat exchanger optimum, can be considered to optimum geometry and dimensions of regenerator. The 1 dimension flat plat model and porous media model have been constructed and compared with entropy generation, cooling capacity, coefficient of performance by changing plate thickness and sphere size at frequency 0.25Hz, 0.5Hz, 1, aspect ratio 2, 7, 14. The result shows that the optimized sphere size will be around 0.2mm to 0.3mm. On the other hand, 0.1mm to 0.2mm thickness plate will be more efficient. Compared the 2 models, flat plate model can get a smaller entropy generation and achieve a higher cooling capacity.

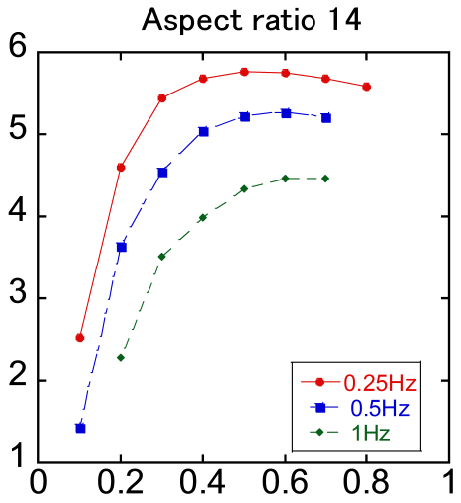

Figure 4-23: COP corresponding to the different particle size at frequency 0.25Hz, 0.5Hz, 1Hz and ascpet ratio 14 in the porous media model.

4.7 Comparison of packed sphere and flat plate regenerator keeping A_s as constant

4.7.1 Results and discussion

The packed sphere model is favored by lower cost and simplicity of construction. If the fabrication problem for flat plate can be solved and plate can be made very thin, we want to know which regenerator can provide a better performance. The performance of the two regenerators have been compared while they have the same heat transfer surface area.

Figure 4-24, 4-25, 4-26,and 4-27 show the entropy generation corresponding to the different sphere size and plate thickness at frequency 1Hz in both flat plate regenerator and packed sphere regenerator. It is found that increased sphere size and plate thickness will increase entropy, especially in packed sphere regenerator. Total entropy generation in packed sphere regenerator is 4 to 6 times of that in flat plate regenerator. In flat plate regenerator, Entropy generation except due to axial thermal conductivity of the regenerator material is smaller than that of packed sphere

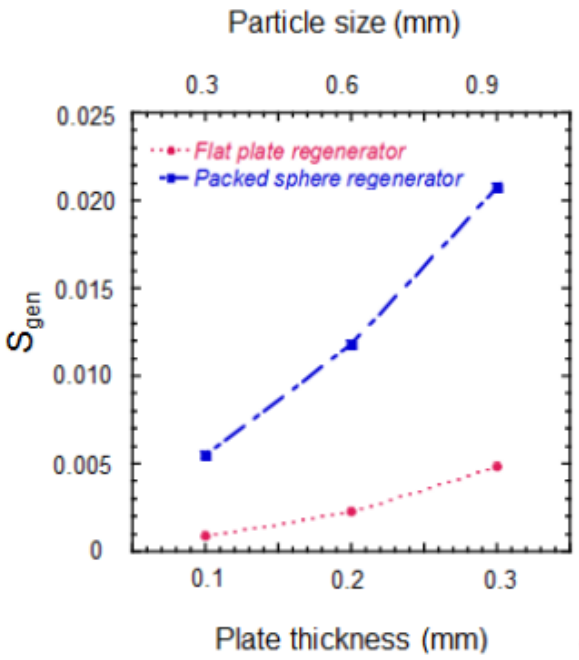

Figure 4-24: Total Entropy generation corresponding to the different plate thickness and sphere size and at frequency 1Hz in both flat plate regenerator and packed sphere regenerator.

regenerator. Entropy generation mainly caused by Finite heat transfer between material and fluid. Entropy generation due to viscous dissipation of the flow energy is significant increased when the sphere size is becoming smaller. Cooling capacity and coefficient corresponding to the different sphere size and plate thickness at frequency 1Hz in both flat plate regenerator and packed sphere regenerator are showed in Figure 4-28 4-29. In Figure 4-28, flat plate regenerator can get 10% to 30% more cooling capacity than that of packed sphere generator. In Figure 4-29 COP of flat plate regenerator can be 30% higher than that of Packed sphere regenerator. Flat plate regenerator has a potential to make AMR more powerful and efficient.

4.7.2 Conclusions

We have successfully compared the two regenerators when they have the same heat transfer surface area and found that flat plate regenerator has a potential to make AMR more powerful and efficient. It can get 10% 30% more cooling capacity and 30% higher COP than that of Packed sphere regenerator.The high performance and

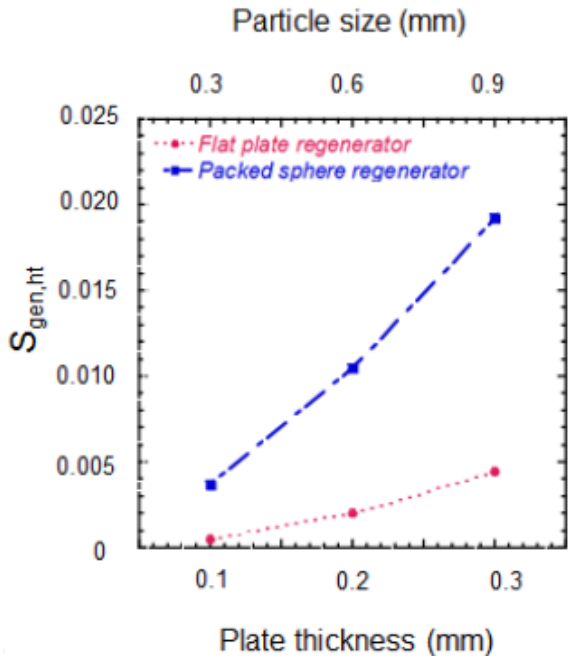

Figure 4-25: Entropy generation due to finite heat transfer corresponding to the different plate thickness and sphere size and at frequency 1Hz in both flat plate regenerator and packed sphere regenerator.

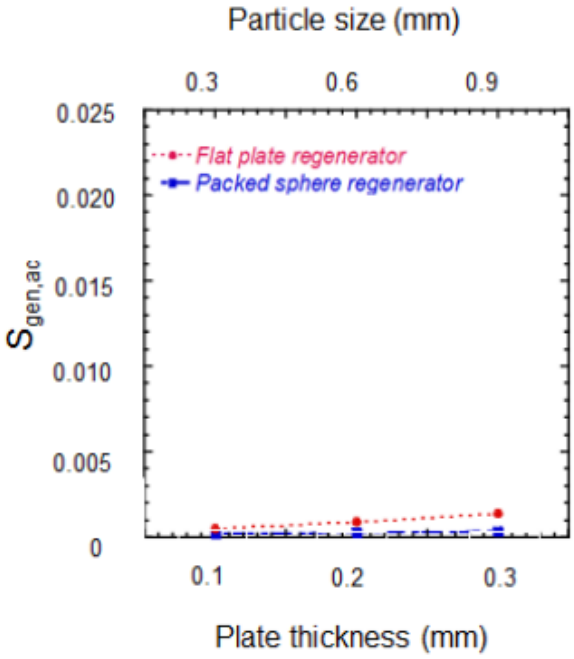

Figure 4-26: Entropy generation due to axial thermal conductivity of the regenerator material corresponding to the different plate thickness and sphere size and at frequency 1Hz in both flat plate regenerator and packed sphere regenerator.

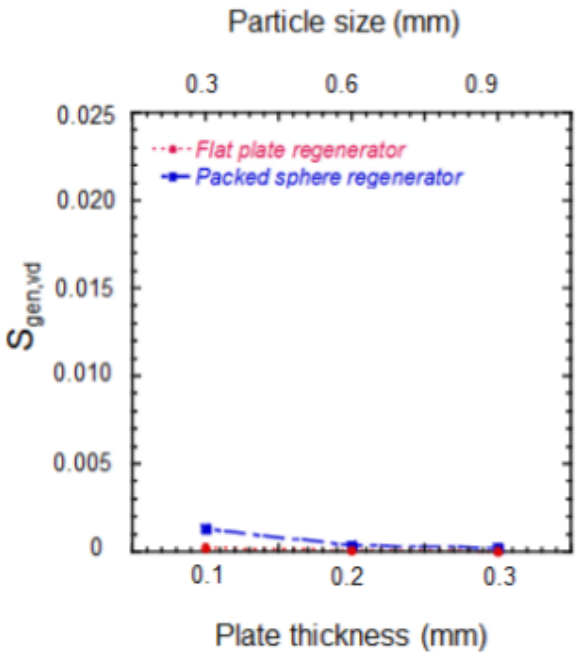

Figure 4-27: Due to viscous dissipation of the flow energy corresponding to the different plate thickness and sphere size and at frequency 1Hz in both flat plate regenerator and packed sphere regenerator.

less entropy generation makes it a promising candidate for AMR system.

4.8 Comparison of Micro-channel, porous media and flat plate regenerator

4.8.1 Results and discussion

Table 4.2 presents the given parameters in numerical modeling. Considering MR relies on MCE, and the mass of Gd can significantly influence the performance of the cooling system, the models have been compared with the same Gd mass. According to previous calculation , frequency is set to 1 Hz which is widely used in prototype AMR to achieve a good performance. Since the material mass is kept constant, different porosity will result in different regenerator volume. The porosity value is fixed to 0.365, which is the biggest porosity used in experimental packed sphere AMR so far. The aspect ratio is set to7 based on an experimental result.

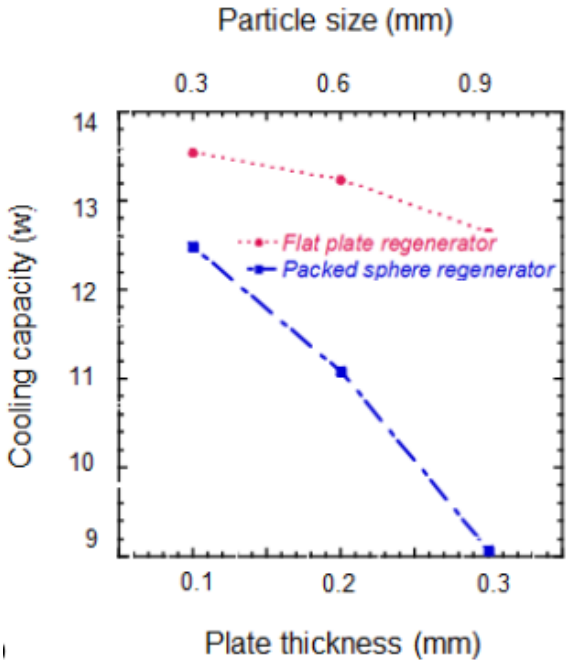

Figure 4-28: Cooling capacity corresponding to the different plate thickness and sphere size and at frequency 1Hz in both flat plate regenerator and packed sphere regenerator.

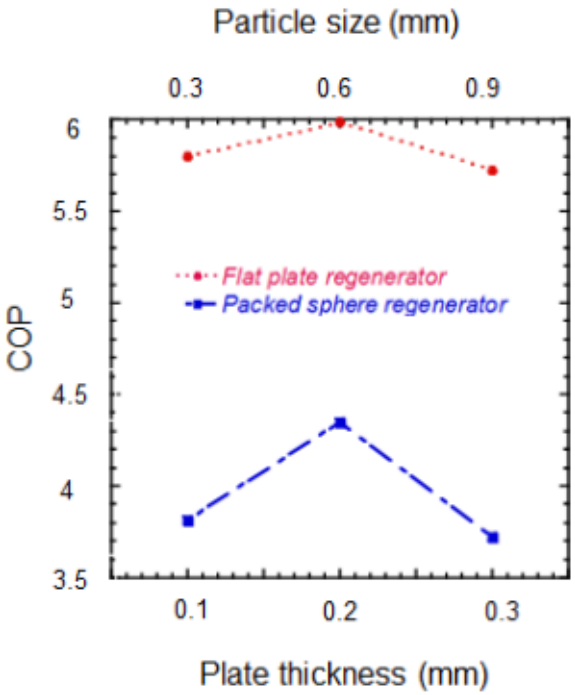

Figure 4-29: COP corresponding to the different plate thickness and sphere size and at frequency 1Hz in both flat plate regenerator and packed sphere regenerator.

Table 4.2: Summary of numerical modeling given parameters

magnetic material	Gd	frequency	1
Fluid	water and ethanol mixture	Aspect ratio	7
Total material mass	0.16kg	Mass flow rate	0.007kg/s
Regenerator size	$20.312cm^3$	Porosity of matrix	0.356
B_{max}	1.2T	T_H	307K
B_{min}	0T	T_L	267K

Figure 4-30, 4-31 and 4-32 shows the variation of cooling capacity and NTU in three regenerators as a function of plate thickness. For the flat plate regenerator in Figure 4-30, the cooling capacity increases as the plate thickness decreases. The maximum cooling capacity is 13.7 W when plate thickness is 0.05mm and NTU is about 1400. When plate thickness increased to 0.1 mm, NTU decreased to about 600 and cooling capacity reduced slightly. For packed sphere regenerator in Figure 4-31, maximum cooling capacity is 12.75 W when particle size is 0.3 mm and NTU is 168. For the micro-channel regenerator in Figure 4-32, cooling capacity increases rapidly when width of micro-channel c decrease from 0.3 mm to 0.03 mm. The maximum cooling capacity is 13 W when c is 0.03mm and NTU is about 230. By comparing the cooling capacity of the three different models, flat plate regenerator can generate 5% more cooling capacity than the micro-channel regenerator and 7% more cooling capacity than the packed sphere regenerator.

Figure 4-33, 4-34 and 4-35 show the variation of COP and FOM in 3 regenerators. In all regenerators, an optimized COP and FOM can be obtained. For flat plate regenerator in Figure 4-33, the maximum COP and FOM are 2.92 and 0.43 when plate thickness is 0.15mm.For packed sphere regenerator in Figure 4-34, the maximum COP is 3.06 when particle size is 0.3mm and FOM is 0.53 when particle size is 0.2mm. For micro-channel regenerator in Figure 4-35, the maximum COP and FOM are 1.43 and 0.22 when c is 0.1mm. Depending on these data, packed sphere and flat plat regenerator have almost the same maximum COP, and the entropy loss of packed sphere regenerator is less than other two models for the bigger FOM.

Figure 4-36, 4-37, 4-38 analyzed the variation of total Entropy Generation (S_total),

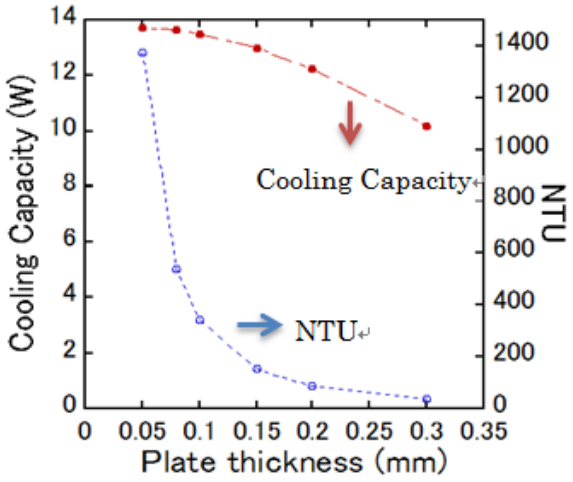

Figure 4-30: Variation of Cooling capacity and NTU in 0.05 mm 0.3 mm plate thickness.

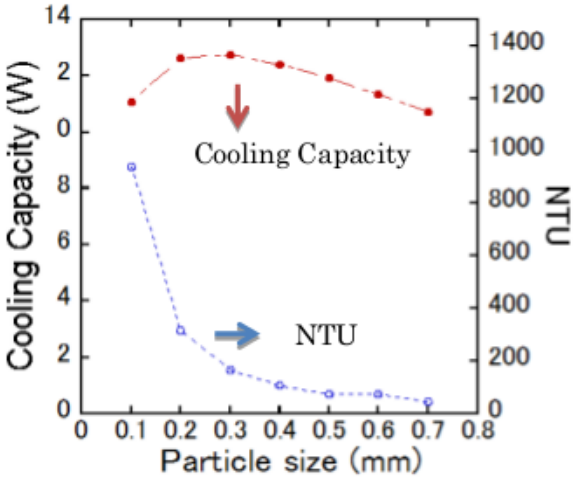

Figure 4-31: Variation of Cooling capacity and NTU in 0.1 mm 0.7 mm particle size packed sphere regenerator.

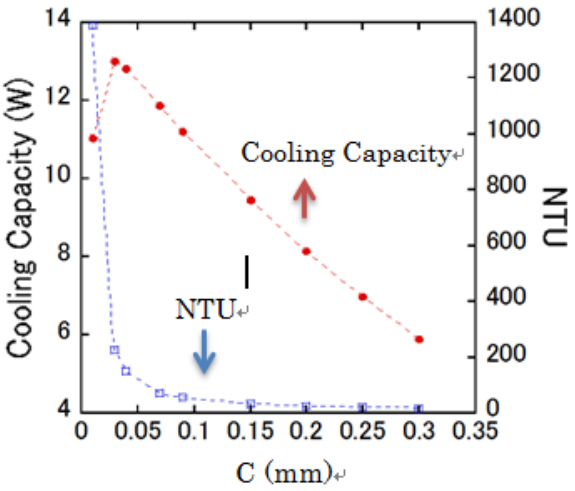

Figure 4-32: Variation of Cooling capacity and NTU in 0.01 mm 0.3 mm width of micro-channel regenerator.

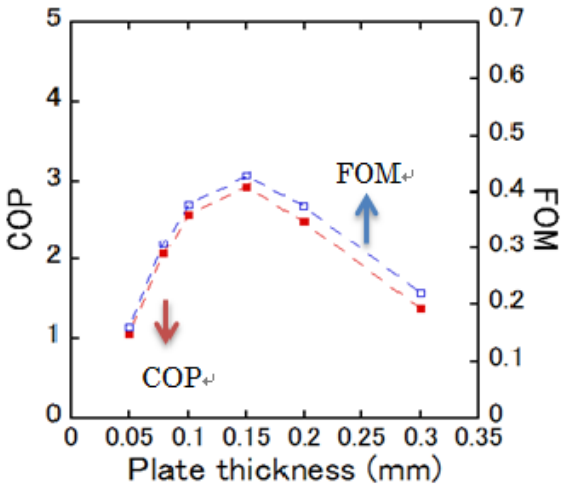

Figure 4-33: Variation of COP and FOM in 0.05 mm 0.3 mm plate thickness.

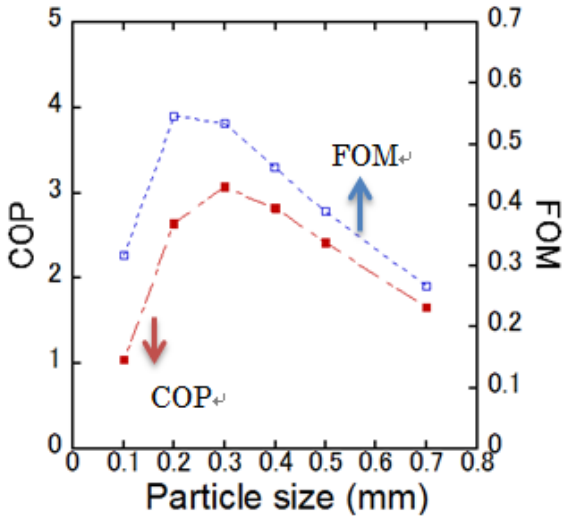

Figure 4-34: Variation of COP and FOM in 0.1 mm 0.7 mm particle size packed sphere regenerator.

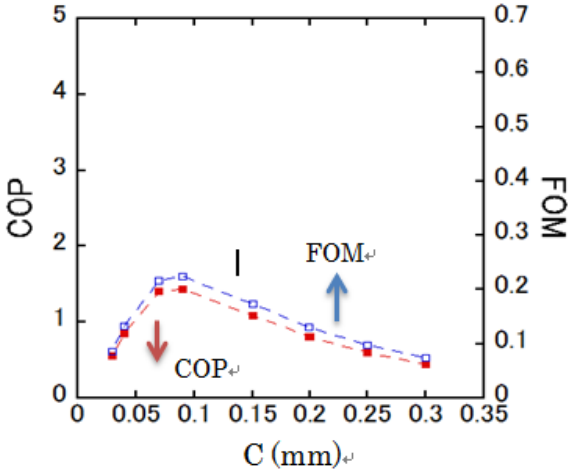

Figure 4-35: Variation of COP and FOM in 0.01 mm 0.3 mm width of micro-channel regenerator.

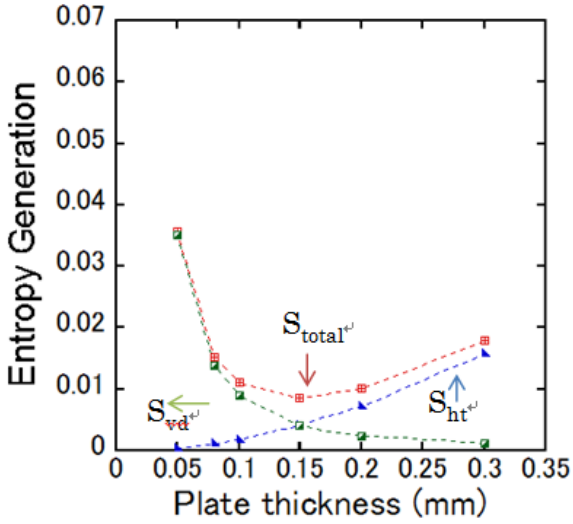

Figure 4-36: Variation of Total EG, EG due to heat transfer and EG due to pressure drop in 0.05 mm 0.3 mm plate thickness.

Entropy Generation (EG) due to heat transfer (Sht) and EG due to pressure drop (Svd) in three regenerators. EG due to axial dissipation is very small and thus negligible. There is a balance point where the combination of Sht and SvdS is smallest. Micro-channel regenerator produces the biggest EG of the three regenerators. By comparing 3 regenerators with both cooling capacity and COP, packed sphere and flat plate regenerator should be more favorable. In the modeling, packed sphere regenerator has been modeled as uniform, and therefore, the pressure drop is much smaller than that of real device operation. So the experimental COP should be smaller than the simulation result. Flat plate regenerator has the potential to have a more efficient performance because of its uniform geometry.

The low efficiency of the flat plate regenerator is partly due to limited heat transfer surface area. Figure 4-39, 4-40 shows the comparison of performance between the existing and idea flat plate regenerator when the plate thickness is from 0.2 to 0.4 mm. The heat transfer surface of idea one is 10 times bigger than that of existing one. Cooling capacity in Figure 4-39 has been improved from 8% to 80% . COP in Figure 4-40 has increased from 100% to 300% and the maximum COP is 4.82 which has been improved 65% and can reach 73% COP_{Carnot}.

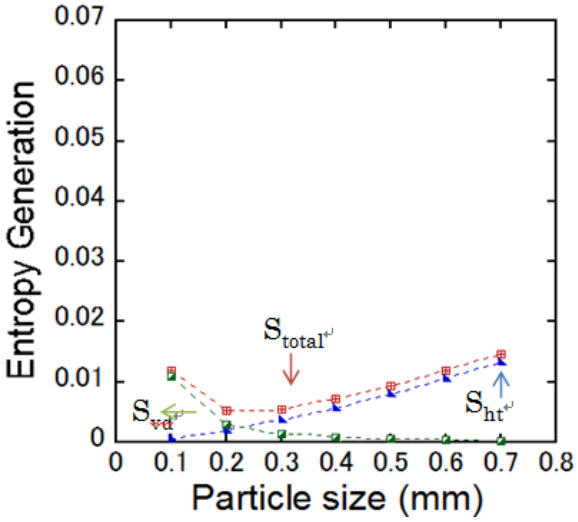

Figure 4-37: Variation of Total EG, EG due to heat transfer and EG due to pressure drop in 0.1 mm 0.7 mm particle size packed sphere regenerator.

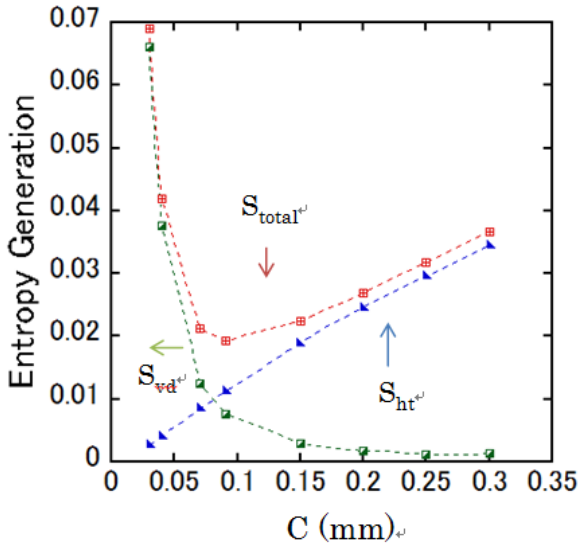

Figure 4-38: Variation of Total EG, EG due to heat transfer and EG due to pressure drop in 0.01 mm 0.3 mm width of micro-channel regenerator.

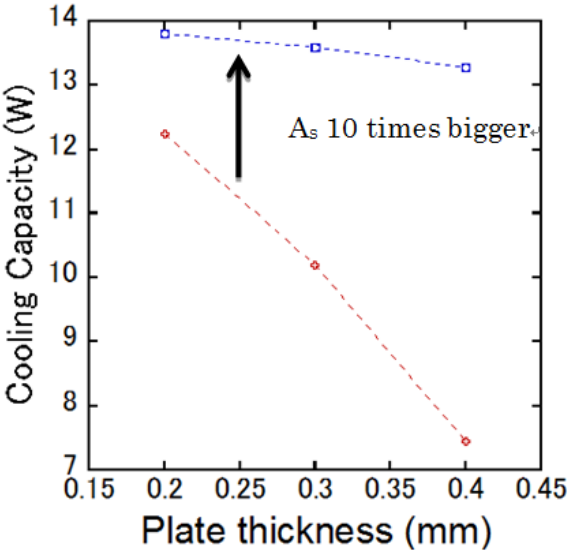

Figure 4-39: Variation of cooling capacity in 0.2 mm 0.4 mm plate thickness flat plate regenerator for different heat transfer surface area.

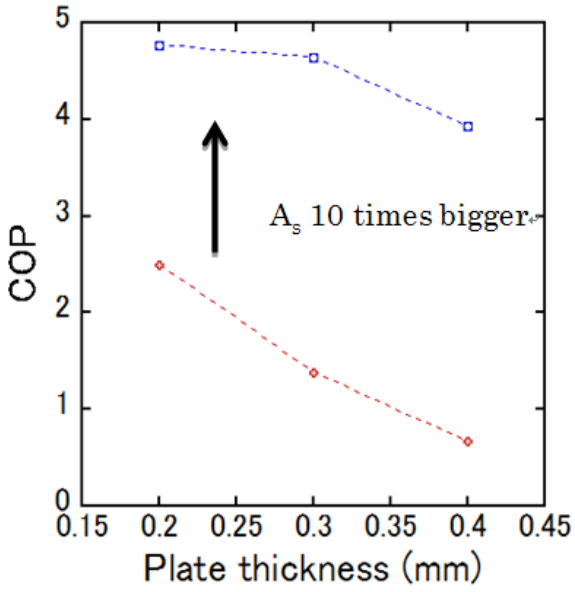

Figure 4-40: Variation of COP in 0.2 mm 0.4 mm plate thickness flat plate regenerator for different heat transfer surface area.

4.8.2 Conclusions

Based on the discussion above, the difference of maximum cooling capacity among three regenerators is not significant. By comparing both cooling capacity and COP, micro-channel is not recommended to be the prototype AMR system due to its big entropy generation and small COP even without considering the inlet and outlet regenerator loss. Packed sphere regenerator geometry shows good performance which is very close to flat plate regenerator. However, the experimental result might be smaller for the non-uniform porosity case, which has a larger loss due to its in homogeneity. Flat plate regenerator has a potential to be even more efficient, which is also suggested by JakaTusek [19]. After expanding the limited heat transfer surface by 10 times, COP can be improved by 65%. Our group will further improve it experimentally with a new technology to increase heat transfer surface area.

Chapter 5

Idea MCE for Optimum AMR Regenerator

AMR is considered to be a device that could be used to produce efficient and compact cooling over a broad range of temperatures. The heart part of AMR is the regenerator which exploits the magnetocaloric effect (MCE). The MCE is the property exhibited by some materials whereby the magnetic field change will cause the heat entropy change. By using such a material in a regenerator as a refrigerant working with heat transfer fluid together, AMR is a new challenge comparing to the traditional refrigeration technology.To understand AMR, the MCE is a key parameter to maximize the cooling performance and suitable temperature span. Maximize the cooling performance is a fundamental question since the AMR was created. The idea of multi-layered regenerator has been proposed in order to strengthen the MCE in a board temperature span. However it is still a problem that how to select and arrange materials in a multi-layered regenerator. In this chapter,to increase our understanding of AMR thermodynamics, we investigated the function of MCE, the influence of the entropy change and operational temperature span to performance. We believe that finding an idea MCE is a necessary step for muliti-layered regenerator to select and arrange materials.

Figure 5-1: MPMS measure magnetization equipment

5.1 Experimental measurement of magnetization

Before the investigation of MCE to performance, experiments to measure magnetization were performed to obtain the entropy change curves of the materials. MPMS measure magnetization equipment has been used which is showed in Figure 5-1. Equation 5-1 has been used to Obtain the entropy curves of the materials from magnetization. Measurements were carried out on sphere Gadolinium (Gd), which is commonly used in room-temperature magnetic refrigeration, with a magnetic field of 1T5T. The parameters of Gd used for measurement are showed in Table . The results are showed in Figure 5-2. The dependences on the temperature and on the magnetic field for Gd as well as the existence of the Curie temperature in the neighborhood of 295K were confirmed.

$$\mathrm{S} = \int_0^H \left(\frac{\partial M}{\partial T} \right) \mathrm{H} \tag{5.1}$$

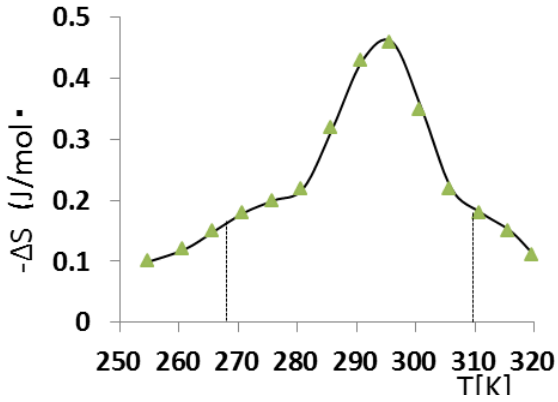

Figure 5-2: Entropy curve of Particle Gd in 1 Tesla

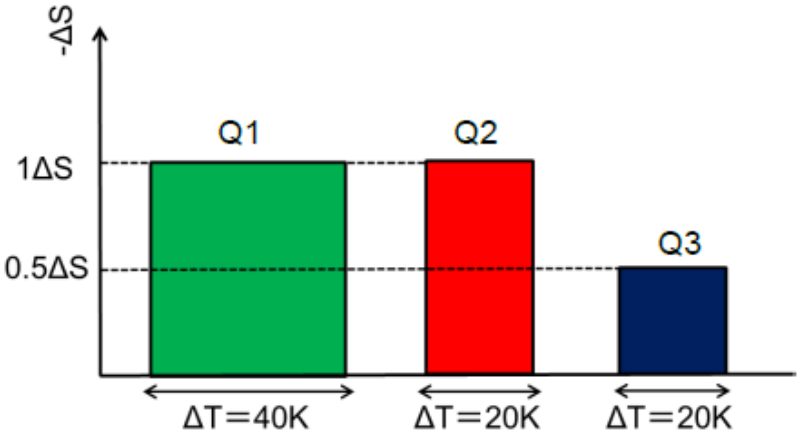

Figure 5-3: Three hypothetical multi-layer regenerators

5.2 Influence of Entropy change and operational temperature span to performance

Entropy change with the temperature variation shows the MCE of material. In order to investigate the influence of entropy change and operational temperature span to performance, three hypothetical multi-layered regenerators have been constructed (Figure 5-3). The green regenerator arranged by materials of $1\Delta S$ entropy change in 40K temperature span. The red regenerator arranged by materials of $1\Delta S$ entropy change in 20K temperature span. The blue regenerator arranged by materials of $0.5\Delta S$ entropy change in 20K temperature span.

Heat generated by material, which is also the MCE of material, can be calculated

Table 5.1: Giving parameters in the comparison of hypothetical regenerators

frequency	1 Hz
Fluid	water and ethanol mixture
Total material mass	0.16kg
magnetic field	1T
T_{high} in δT40K	313K
T_{low} in δT40K	273K
T_{high} in δT20K	293K
T_{high} in δT20K	273K

by a well known relation as follow:

$$Q = \Delta S \Delta T \tag{5.2}$$

Based on Equation 5.2

$$Q_1 = 2Q_2 = 4Q_3 \tag{5.3}$$

Q_1 is the heat generated by the green regenerator. Q_2 is the heat generated by the red regenerator. Q_3 is the heat generated by the blue regenerator.

5.2.1 Results and discussion

Three regenerators will be compared in one dimensional packed media modeling.In three regenerators, the data of material character excepting MCE are based on sphere Gd. Q2, the MCE in the red regenerator, equals to the MCE of sphere Gd in the magnetic field of one Tesla in the exactly same fixed operation temperature span. Other giving parameters in the comparison simulation are giving in Table 5.1.

In Figure 5-4, the red and blue regenerator are in the same operational temperature span. The MCE of the green regenerator is the twice of the red one. And the refrigeration performance of the green regenerator showed more than twice bigger than that of the blue one. It is implied that increase entropy change will greatly improve the performance. In Figure 5-5, the red and green regenerator have the same entropy change. And the operatioal temperature span of the green regenerator is twice

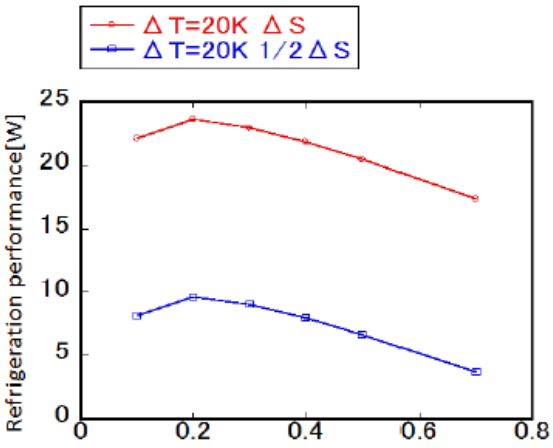

Figure 5-4: The refrigeration performance comparison between the green and red regenerator

of the red one. The comparison results showed that enlarge the operational temperature span will decrease the performance. And twice lager temperature span has not reduced half performance. However,Enlarge the operational temperature span dose not reduce the performance in Figure 5-6. Even the green regenerator is operationed in 40K but also has double entropy change comparing to the blue regenerator. The reults showed that the green regenerator has a better performance. It is implied that Increasing the entropy change can enlarge the operational temperature span. When the operational temperature span is twice larger, it is not required to use double entropy change magnetic material to reach the same cooling performance.

5.2.2 Conclusions

In order to investigate the influence of entropy change and operational temperature span to performance, three hypothetical multi-layered regenerators have been constructed and compared. It is implied that increasing entropy change will greatly improve the performance and enlarge the operational temperature span.

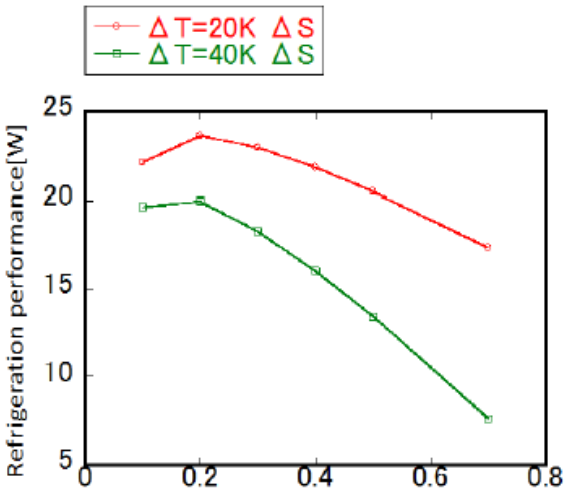

Figure 5-5: The refrigeration performance comparison between the red and blue regenerator

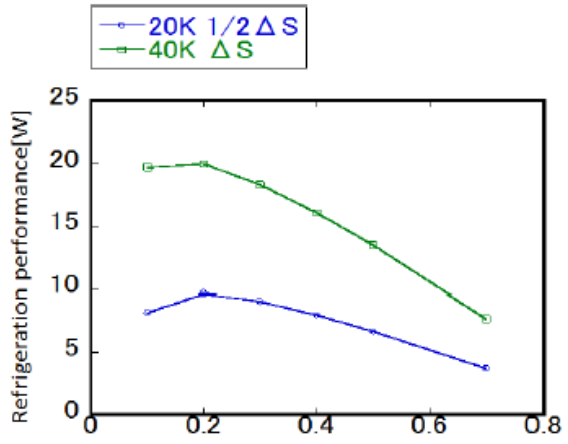

Figure 5-6: The refrigeration performance comparison between the green and blue regenerator

5.3 Optimization of MCE

5.3.1 Themordynamic requirements

An early themordynamic requirements analysis of the AMR regenerator have been proposed by Cross et al [5].The analysis are based on the entropy generation minimization.They found the relation of temperature change in material and operational temperature when keeping the entropy flow as constant.Further analysis was performed by Hall et al [11].He suggested that no unique idea MCE exists for the AMR. This parprograph is to investigate idealized AMR regenerator behavior. The heat generated by entropy change and operational temperature can be caculated by Equation 5-2. According to the first law of the thermodynamics for a reversible system, the relation of heat generated in hot end Q_h and cold end Q_c can be caculated as follow:

$$Q_h = Q_c + W \tag{5.4}$$

By inserting Equation 5.2 in to Equation 5.4, it follows for the ratio of heat in cold and hot end:

$$\frac{Q_h}{Q_c} = \frac{T_h \Delta S_h}{T_c \Delta S_c} \tag{5.5}$$

Setting W=0 which means no work has been done from outside,no heat generated by material itself flow from hot to cold end.Then, the relation of entropy change in hot and cold end is:

$$\frac{\Delta S_c}{\Delta S_h} = \frac{T_h}{T_c} \tag{5.6}$$

This relation effectively sets the required entropy change ratio between hot and cold end and sets the optimum T-S profile of the material across the entire temperature range.

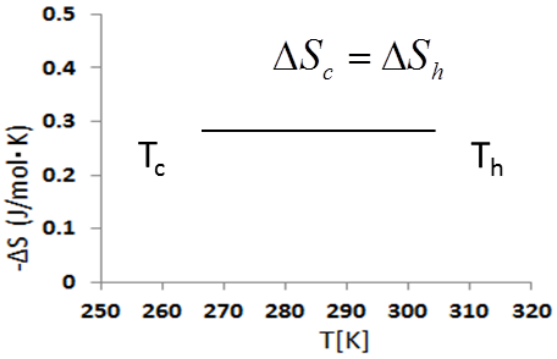

Figure 5-7: Iso-entropy change regenerator

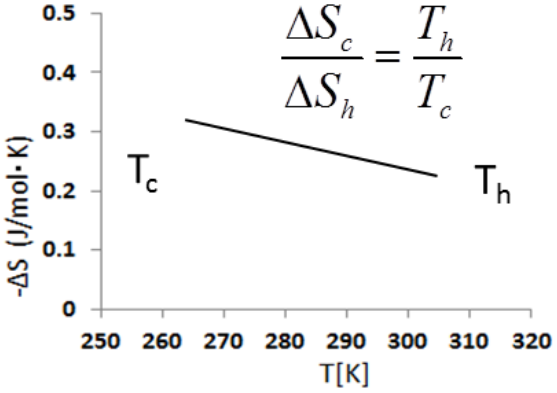

Figure 5-8: Idea entropy change regenerator

5.3.2 Comparison of Single, Iso-entropy change, Idea entropy change regenerator

In order to prove this optimum T-S profile will improve the performance of AMR system. Three types of regenerators will be compared in this paragraph. One is the Gd regenerator which is the most wildly used single regenerator in room temperature. Another is the Iso-entropy change regenerator which is based on the idea MCE proposed by Cross et al [5] (Figure 5-7).The third one is the idea entropy change regenerator where the entropy change ratio is based on Equation 5.6.(Figure 5-8)

Simulation conditions: 1, Three regenerators will be compared in one dimensional packed media modeling. 2, The single regenerator is based on a real material spherical Gd in the magnetic field of one Tesla. 3, The data of material character excepting MCE are all based on sphere Gd in three regenerators. 4, The MCE are kept as a

Table 5.2: Summary of numerical modeling given parameters

magnetic material	Gd	frequency	1
Fluid	water and ethanol mixture	Aspect ratio	7
Total material mass	0.16kg	Mass flow rate	0.007kg/s
Regenerator size	$20.312cm^3$	Porosity of matrix	0.356
B_{max}	1T	B_{min}	0T

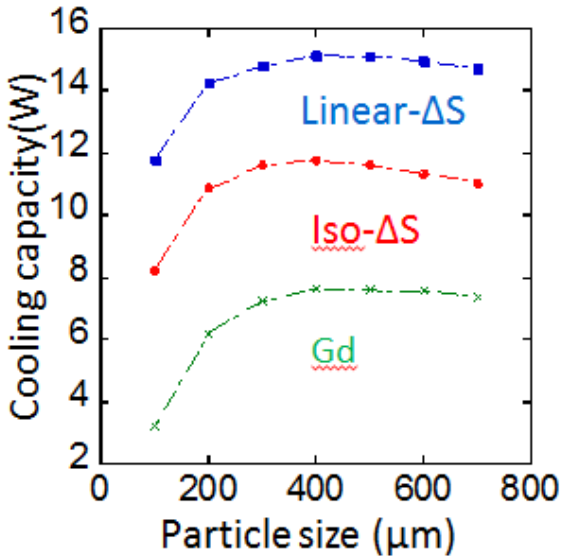

Figure 5-9: Comparison of Single, Iso-entropy curve, Idea entropy curve multi-layered regenerator in cooling capasity in porous media model

constant which are shown in Figure 1, 2, 3 as the red area. 5, Keeping the operation temperature span as constant (Tc=263K, Th=303K). 6, All the other parameters are shown in Table 5.2.

5.3.3 Results and discussion

Both in Figure 5-9 and 5-10, the idea entropy change regenerator showed the best performance. In figure 5-9, the cooling capacity of the idea entropy change regenerator is about double of the single regenerator and 1.5 times of the iso-entropy change regenerator. In figure 5-10, the maximization COP of the idea entropy change regenerator is about double of the single one. The minimization COP of the idea entropy change regenerator is about four times of the single one. The COP of the idea entropy change

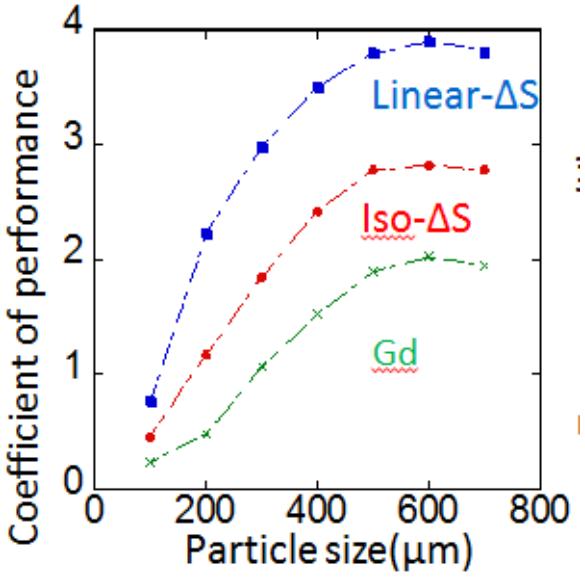

Figure 5-10: Comparison of Single, Iso-entropy curve, Idea entropy curve multi-layered regenerator in COP in porous media model

regenerator can be 1.5 times of the iso-entropy change one. The optimum T-S profile of the material should be used to selet and arrange the magnetic material which will greatly improve the performance.

5.3.4 Conclusions

In order to deeply understand the thermodynamics of AMR, we examine the influenc of MCE (entopy change,operational temperature span) to the performance and the heat balance in an idealized AMR regenerator. An idea MCE which based on the optimum T-S profile for the case of constant heat generated across the regenerator has been proposed.For proving this idea, Single, Iso-entropy change, Idea entropy change regenerator have been compared by one dimentional model. The results showed that the idea entropy change regenerator has a much better performance that other two types regenerators. We believe that this idea MCE will be a guide to select and arrange magnetic material.

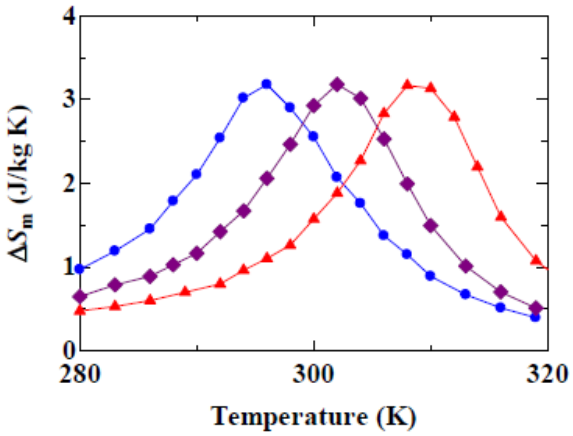

Figure 5-11: Entropy change (δS) depending on Temperature

5.4 Schematic of multi-layer regenerator

The best case for the selection of magnetic material is to use a material which satisfy special requirements of the the optimum T-S profile. However, this idea material has not been found yet. Figure 5-11 shows the temperature dependences of entropy changes for materials with different Curie temperatures. Each material has a large entropy change at curie temperature and the entropy will change with the variation of the temperature.Hashimoto et al [12] suggested using multi-layer magnetic material comprising layers of different magnetic materials in necessary proportion and arranged in necessary order determined by their ordering temperature. A schematic diagram of layering is shown in Figure 5-12. The schematic of Tishin [20] et al for the first time used the multi-layer regenerator idea using Gd-Tb,Gd-Dy and Tb-Dy. The multi-layer regenerator showed a better performance than the single one. Recently years, the most famours research group about the multi-layer regenerator is the group in Canada. Rowe et al [19] [17]used 2 and 3 materials for the packed media regenerator in room AMR. Figure 5-13 is the schematic diagram from single material regenerator to multi-layer regenerator in packed media regenerator.The partical will be separated by mesh inside the regenerator. However, their results showed that the cooling of the multi-layer regenrators are not always better than the single one. In the near future, the new multi-layer regenerator based on the idea MCE caculated in this chapter will

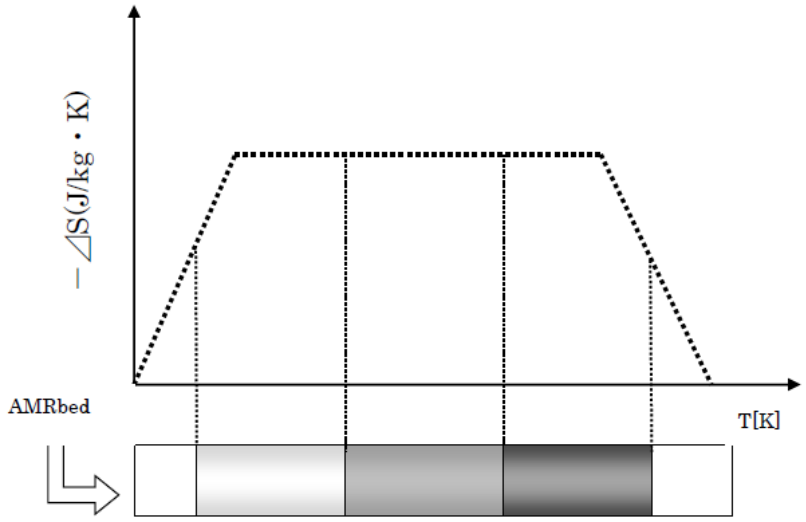

Figure 5-12: Schematic diagram of multi-layer regenerator

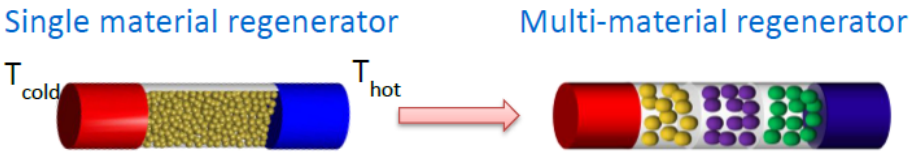

Figure 5-13: Arrangement of different magnetic material in paked sphere regenerator

be constructed and compared with the single material regenertor experimantly.

Chapter 6

Conclusions

In order to commercialize the magnetic refrigeration techonology in room temperature, the magnetic material and system design have to be both improved. In this thesis, we investigated the optimum regenerator which is the heart part in AMR system both from these tow points. The optimization of regenerator geometry is to improve the cooling system design.The investigation of Idea MCE is in order to select and arrange magnetic material efficiently.The purpose of this thesis is to find the idealized AMR regenerator.The knowledge of fundamental physics, mechanical engineering and computer science for builting complex modeling have been used.

In the part of regenerator geometry design, the entropy generation minimization method has been used to compare the different geometry regenerators and minimize the entropy generation generated during the AMR cycle. The following conclusions can be drawn:

1,The first porous media 2-dimensional and micro-channel model have been constructed which have been used to analyze the heat process of the regenerators. The 2-D model and the previous 1-D model were compared. It is concluded that the loss caused by air convection and the conduction loss in y-axis can not be ingnored. The 2-dimention porous media model can better predict the performance of cooling system. 2,Influence of Frequency, Aspect ratio, Heat transfer surface have been analyzed in flat plate, porous media and micro-channel regenerator.It is found that high velocity can make the heat transfer rate higher for the different regenerator geometries. Thus,

a high operation frequency is needed to improve the cooling capacity. In high velocity field, flat plate model is better than porous media model for the better heat transfer to pressure drop ratio. 3,Entropy generation minimization method has been used to optimize the real devices and processes.Indeed this method is showing a good way to deeply understand the thermodynamic process during the cycle. 3,Flat plate regenerator is suggested for the potential regenerator.Micro-channel is not recommended to be the prototype AMR system due to its big entropy generation and small COP even without considering the inlet and outlet regenerator loss. Packed sphere regenerator geometry shows good performance which is very close to flat plate regenerator. However, the experimental result might be smaller for the non-uniform porosity case, which has a larger loss due to its in homogeneity. 4,Increase heat transfer surface area with a new technology is numerically proved to be a good method to significantly improve the cooling performance. The realization of this idea is considered to use a new nano-techonology to achieve. Further more investigation is needed.

In the part of idea MCE for AMR regenerator, the thermodynamic requirement has been performed.The optimum T-S profile of the material for the idea MCE has been used to construct a new multi-layered regenerator. Different types of regenerators and single regenerator have been compared. The following conclusions can be draw: 1, The influence of entropy change and operational temperature span have been examed. It is implied that increasing entropy change will greatly improve the performance and enlarge the operational temperature span. 2, An idea MCE which based on the optimum T-S profile for the case of constant heat generated across the regenerator has been proposed.For proving this idea, Single, Iso-entropy change, Idea entropy change regenerator have been compared by one dimentional model. The results showed that the idea entropy change regenerator has a much better performance that other two types regenerators. 3,The idea MCE will be a guide to select and arrange magnetic material.The new multi-layer regenerator based on the idea MCE need to be constructed experimantly.

These results indicate that the exited regenerator design and single regenerator are not efficient.The new technology and idea have to be considered.The idea MCE

regenerator presented is a good instrument to design a prototype of a multi-layered regenetor.

Chapter 7

Acknowledgement

Completion of this doctoral dissertation was possible with the support of several people. I would like to express my sincere gratitude to all of them.

First of all, I am extremely grateful to my research guide, Professor Nakagome, for his valuable guidance, scholarly inputs and consistent encouragement I received throughout the research work.

This feat was possible only because of the unconditional support provided by Dr.Numazawa with an amicable and positive disposition, Sir has always made himself available to clarify my doubts despite his busy schedules and I consider it as a great opportunity to do my doctoral programme under his guidance and to learn from his research expertise. Thank you Sir, for all your help and support.

Professor Mastumoto, has been very encouraging and supportive, and thank him for his valuable suggestions and concise comments on some of the research papers.

I would like to thank my thesis committee, Prof.Otsubo, Prof. Maeno and Associate Prof. Wajima for their direction, dedication, and invaluable advice.

I am grateful to Dr.Yanagizawa, for his suggestions in research and helpful discussion. I also thank Zhu yiyin, for her support in material data analysis.

I acknowledge my reserch group members, Mr.Hirano, Mr.Hatori, Mr.Sonoda, Mr.Ueda, for being the accompany for my doctoral course.

The thesis would not have come to a successful completion, without the help I received from Mrs.Sugioka. I thanks and appreciate her efforts.

In the last Five years, I was doing research in National Institutef for Material Science(NIMS).Thanks NIMS for the academic support and the facilities provided to carry out the research.

Finally, I would like to thank my parents. I owe a lot to my parents, who encouraged and helped me at every stage of my personal and academic life, and longed to see this achievement come true. I deeply miss my mother Cheng dongjie, who is not in Japan with me to share this joy. My father Li caixiang, who is my life advisor and a great supporter during the field study.

Bibliography

[1] John A Barclay and Sunil Sarangi. Selection of regenerator geometry for magnetic refrigerator applications. Technical report, Los Alamos National Lab., NM (USA), 1984.

[2] Steyert W.A. Barclay, J.A. Active magnetic regenerator, 1982.

[3] G. V. Brown. Magnetic heat pumping near room temperature. *Journal of Applied Physics*, 47(8), 1976.

[4] A. Sternberg V.K. Pecharsky K.A. Gschneidner Jr. M. Osborne I. Anderson C. Zimm, A. Jastrab, editor. *Description and performance of a near-room temperature magnetic refrigerator*, volume 43 of *Advances in Cryogenic Engineering*, 1998.

[5] CR Cross, JA Barclay, AJ DeGregoria, SR Jaeger, and JW Johnson. Optimal temperature-entropy curves for magnetic refrigeration. In *Advances in Cryogenic Engineering. Volume 33*, volume 33, pages 767–775, 1988.

[6] P. Debye. *Ann. Phys*, 81:1154, 1926.

[7] Kurt Engelbrecht. Thesis (m.s.):a numerical model of an active magnetic regenerator refrigeration system.

[8] Kurt Engelbrecht, Christian Robert Haffenden Bahl, and Kaspar Kirstein Nielsen. Experimental results for a magnetic refrigerator using three different types of magnetocaloric material regenerators. *International Journal of refrigeration*, 34(4):1132–1140, 2011.

[9] W. F. Giauque. *J. Am. Chem. Soc*, 49:1870, 1927.

[10] W. F. Giauque and D. P. MacDougall. Attainment of temperatures below. *Phys. Rev.*, 43:768–768, May 1933.

[11] JL Hall, CE Reid, IG Spearing, and JA Barclay. Thermodynamic considerations for the design of active magnetic regenerative refrigerators. In *Advances in cryogenic engineering*, pages 1653–1663. Springer, 1996.

[12] T Hashimoto, T Kuzuhara, M Sahashi, K Inomata, A Tomokiyo, and H Yayama. New application of complex magnetic materials to the magnetic refrigerant in an ericsson magnetic refrigerator. *Journal of applied physics*, 62(9):3873–3878, 1987.

[13] M Kaviany. Principles of heat transfer in porous media, springer, new york, 1995.

[14] V. K. Pecharsky and K. A. Gschneidner, Jr. Giant magnetocaloric effect in. *Phys. Rev. Lett.*, 78:4494–4497, Jun 1997.

[15] XF Peng and GP Peterson. Convective heat transfer and flow friction for water flow in microchannel structures. *International Journal of Heat and Mass Transfer*, 39(12):2599–2608, 1996.

[16] G. Courret P.W. Egolf, O. Sari, editor. *Trends of refrigeration and air conditioning technology in Europe*, Proceedings of the Japanese Conference on Cold and Air Conditioning, Okaya, 2002. Japanese Society of Refrigerating and Air Conditioning Engineers (JSRAE). Invited paper: 19.

[17] M-A Richard, AM Rowe, and R Chahine. Magnetic refrigeration: Single and multimaterial active magnetic regenerator experiments. *Journal of applied physics*, 95(4):2146–2150, 2004.

[18] Warren M Rohsenow, James P Hartnett, Young I Cho, et al. *Handbook of heat transfer*, volume 3. McGraw-Hill New York, 1998.

[19] A Rowe and A Tura. Experimental investigation of a three-material layered active magnetic regenerator. *International journal of refrigeration*, 29(8):1286–1293, 2006.

[20] AM Tishin. Magnetic refrigeration in the low-temperature range. *Journal of applied physics*, 68(12):6480–6484, 1990.

[21] Armando Tura. Energetic performance of regenerators in an active magnetic refrigerator. 2012.

[22] Jaka Tušek, Andrej Kitanovski, and Alojz Poredoš. Geometrical optimization of packed-bed and parallel-plate active magnetic regenerators. *International Journal of Refrigeration*, 2013.

[23] Noriaki Wakao and Seiichirō Kagei. *Heat and mass transfer in packed beds*, volume 1. Taylor & Francis US, 1982.

[24] B.F Yu, Q Gao, B Zhang, X.Z Meng, and Z Chen. Review on research of room temperature magnetic refrigeration. *International Journal of Refrigeration*, 26(6):622 – 636, 2003.

[25] C. Zimm, A. Boeder, J. Chell, A. Sternberg, A. Fujita, S. Fujieda, and K. Fukamichi. Design and performance of a permanent-magnet rotary refrigerator. *International Journal of Refrigeration*, 29(8):1302 – 1306, 2006.

PUBLICATIONS AND CONFERENCES

Publications

.

1. J.Li*, T. Numazawa, K.Matsumoto, H. Nakagome, "Numerical modeling on a reciprocating active magnetic regenerator refrigeration in room temperature," *Cryocooler 16, ICC press,* p.536-540(2010)
2. Li J*, T. Numazawa, K.Matsumoto, H. Nakagome, "Numerical modeling on a reciprocating active magnetic regenerator refrigeration in roomtemperature," *Cryogenics, Volume 51, Issue 6,* p.347-352(2011)
3. J.Li* , T. Numazawa, K.Matsumoto, H. Nakagome, "A Modeling study on the Geometry of Active Magnetic Regenerator," *ADVANCES IN CRYOGENIC ENGINEERING: Transactions of the Cryogenic Engineering Conference - CEC, Volume 57,* p.327-334(2011)
4. Li J* , T. Numazawa, K.Matsumoto, H. Nakagome, "A modeling study on the geometry of AMR regenerator: Comparison of Flat plate and Packed sphere regenerator," *ICEC24-ICMC2012 proceedings,* p.223-226 (2012)
5. Li J* , T. Numazawa, K.Matsumoto, H. Nakagome, "Comparison of different regenerator geometries for AMR system," *ADVANCES IN CRYOGENIC ENGINEERING: Transactions of the Cryogenic Engineering Conference - CEC,* accepted (2013)
6. Yiyin Zhu, Jing Li* et al., "Numerical Simulation for Hydrogen Magnetic Refrigeration," *ADVANCES IN CRYOGENIC ENGINEERING: Transactions of the Cryogenic Engineering Conference - CEC, Volume 57,* p.327-334(2011)
7. Hattori H.,Hirano Y.,Wang p.,LI Jing* et al., "Development of AMR hydrogen magnetic refrigeration equipment by external gas driven," *Cryogenics and Superconductivity Society of Japan,* 1C-a04, p.50 (2010)

Conferences

· Jing Li* et al., " Numerical modeling on an Active Magnetic Regenerator Refrigeration," *Asian Conference on Applied Superconductivity and Cryogenics,* Matsue, Japan (2009)

· Jing Li* et al., "Numerical modeling on a reciprocating active magnetic regenerator refrigeration in room temperature," *International Cryocooler Conference 16,* Atlanta, GA, USA (2010)

· Hattori H.,Hirano Y.,Wang p.,LI Jing* et al., "Development of AMR hydrogen magnetic refrigeration equipment by external gas driven, " *Cryogenics and Superconductivity Society of Japan,* 1C-a04, Kagoshima, Japan (2010)

· LI Jing* et al., "A Modeling study on the Geometry of Active Magnetic Regenerator, " *Cryogenics and Superconductivity Society of Japan,* 1C-a05, Kagoshima, Japan (2010)

· Jing Li* et al., " A Modeling study on the Geometry of Active Magnetic Regenerator," *Cryogenic Engineering Conference and the International Cryogenic Materials Conference,* C1OrH-01, Spokane, WA, USA (2011)

· Y. Zhu, J. Li* et al., " Numerical modeling on an Active Magnetic Regenerator Refrigeration," *Cryogenic Engineering Conference and the International Cryogenic Materials Conference,* C1OrH-02, Spokane, WA, USA (2011)

· LI Jing* et al., "A Modeling study on the Geometry of Active Magnetic Regenerator," *Cryogenics and Superconductivity Society of Japan,* 3D-a08, Kanazawa, Japan (2011)

· Jing Li* et al., " A modeling study on the geometry of AMR regenerator: Comparison of Flat plate and Packed sphere regenerator ," *24th International Cryogenic Engineering Conference-International Cryogenic Materials Conference,* Fukuoka, Japan (2012)

· Jing Li* et al., " A simulation of single and multimaterial AMR regenerator," *International Cryocooler Conference 17,* Los Angles, CA,USA (2012)

· Jing Li* et al., "Comparison of different regenerator geometries design for magnetic refrigeration system," *Cryogenics and Superconductivity Society of Japan,* 2D-a03, Tokyo, Japan (2013)

· Jing Li* et al., "Comparison of different regenerator geometries for AMR system," *Cryogenic Engineering Conference and the International Cryogenic Materials Conference,* Anchorage, ALaska,USA (2013)